

Power, energy, and spectrum of a naked singularity explosion

Tomohiro Harada *

Department of Physics, Waseda University, Ohkubo, Shinjuku, Tokyo 169-8555, Japan

Hideo Iguchi †

*Department of Earth and Space Science, Graduate School of Science, Osaka University,
Toyonaka, Osaka 560-0043, Japan*

Ken-ichi Nakao ‡

Department of Physics, Osaka City University, Osaka 558-8585, Japan

It is well known that a naked singularity occurs in the gravitational collapse of an inhomogeneous dust ball from an initial density profile which is physically reasonable. In this paper we show that explosive radiation is emitted during the formation process of the naked singularity while we fix the background spacetime. The energy flux is proportional to $(t_{\text{CH}} - t)^{-3/2}$ for a minimally coupled massless scalar field, while it is proportional to $(t_{\text{CH}} - t)^{-1}$ for a conformally coupled massless scalar field, where $t_{\text{CH}} - t$ is the “remaining time” until the distant observer could observe the singularity if the naked singularity was formed. As a consequence, the radiated energy grows unboundedly for both scalar fields. The amount of the power and energy depends on the parameters which characterize the initial density profile but do not depend on the gravitational mass of the cloud. In particular, there is a characteristic frequency ν_s of the singularity above which the divergent energy is radiated. The energy flux is dominated by particles of which the wavelength is about $t_{\text{CH}} - t$ at each moment. The observed total spectrum is nonthermal, i.e., $\nu dN/d\nu \sim (\nu/\nu_s)^{-1}$ for $\nu > \nu_s$. If the naked singularity formation could continue until a considerable fraction of the total energy of the dust cloud is radiated, the radiated energy would reach about $10^{54}(M/M_\odot)\text{erg}$. The calculations are based on the geometrical optics approximation which turns out to be consistent for a rough order estimate. The analysis does not depend on whether or not the naked singularity occurs in its exact meaning. This phenomenon may provide a new candidate for a source of ultrahigh energy cosmic rays or a central engine of γ -ray bursts.

PACS numbers: 04.20.Dw, 04.70.Dy, 98.70.Sa

I. INTRODUCTION

It was shown that the collapse of an inhomogeneous dust ball results in shell-focusing naked singularity formation [1–4]. Ori and Piran [5–7] and Harada [8] showed that naked singularity formation is possible from the spherical collapse of a perfect fluid with a very soft equation of state. Moreover, a kind of runaway collapse in Newtonian gravity looks like naked singularity formation in general relativity. These strongly suggest that the collapse in the Universe will lead to a drastic growth of spacetime curvature which is not covered by the event horizon.

In this respect, a number of researchers have examined the emission during naked singularity formation. In classical theory, Shapiro and Teukolsky [9,10] reported the drastic growth of a curvature polynomial but no apparent horizon in their numerical simulation of the axisymmetric collapse of a prolate spheroid of collisionless particles. They also reported that little gravitational radiation was emitted in their simulation. On the other hand, Nakamura, Shibata

* Electronic address: harada@gravity.phys.waseda.ac.jp

† Electronic address: iguchi@vega.ess.sci.osaka-u.ac.jp

‡ Electronic address: knakao@sci.osaka-cu.ac.jp

and Nakao [11] suggested that the naked singularity formation in the collapse of a prolate spheroid may provide a strong source of gravitational waves. Recently, Iguchi, Nakao, and Harada [12] and Iguchi, Harada, and Nakao [13,14] examined the behavior of nonspherical linear perturbations of the collapse of an inhomogeneous dust ball. One of their main results is that perturbations of a curvature polynomial grow unboundedly while the energy flux of the gravitational waves remains finite as the Cauchy horizon is approached, which implies that the instability is rather milder.

On the other hand, Hawking [15] showed that thermal radiation is emitted in the gravitational collapse to a black hole. The emission can be interpreted as particle creation due to the time variation of a strong spacetime curvature. In the collapse to a black hole, the magnitude of the spacetime curvature of the observable region is, at most, the order of the inverse square of its gravitational mass because the singularity is covered by the event horizon. On the other hand, in the collapse to naked singularity, the magnitude of the spacetime curvature outside the event horizon grows unboundedly and the strongly curved region can be seen by an observer. This fact suggests that naked singularity formation may be a strong source of emission due to the quantum effect. In this context, Ford and Parker [16] calculated the radiation during the formation process of shell-crossing naked singularity. They found that both the power and the energy remain finite, which is because of the weakness of the shell-crossing singularity. They also showed that the collapse of supercritically charged matter to the naked singularity emits unbounded power and energy, although this spacetime is not a solution of the Einstein equation. Hiscock, Williams and Eardley [17] showed the diverging energy flux in the self-similar collapse of a null dust and also calculated the expectation value of stress-energy tensor in its two-dimensional version. Barve et al. [18] showed the diverging power of radiation in the self-similar collapse of a dust ball. They also calculated the expectation value of stress-energy tensor in its two-dimensional version [19]. Vaz and Witten [20] also calculated the Bogoliubov coefficients which relate to the spectrum of emission for this model. The above studies were all based on the geometrical optics approximation.

The last two examples in which the diverging power is emitted are self-similar collapse. However, the self-similar collapse is a particular solution among gravitational collapse solutions in general relativity. Moreover, we do not know whether or not the central part of the realistic collapse of the nonzero pressure perfect fluid tends to be self-similar in a strong-gravity regime such as a shell-focusing singularity, although such tendency has been observed in the Newtonian regime. For the self-similar collapse of a dust ball, it has been shown that the redshift at the center becomes infinite and that the curvature strength of the naked singularity is very strong. Moreover, it is known that such a solution does not allow the initial density profile which is a C^∞ function with respect to the local Cartesian coordinates. On the other hand, Christodoulou [2] imposed the C^∞ condition on the initial density distribution in his famous paper on the violation of cosmic censorship in the collapse of a dust ball. For the C^∞ case, the redshift is finite and the naked singularity is not very strong. See [21–23] for details. Though the Einstein equation does not require such strong differentiability to initial data, we usually set such initial data in most astrophysical numerical simulations. Although this model is shown to be unstable to nonspherical perturbations, the model is still good for the sufficiently spherically symmetric collapse of dust until the nonspherical perturbations grow sufficiently. It will be important to examine whether or not the divergence of the radiated energy flux in the self-similar collapse only comes from the uniqueness of self-similarity. In this context, the authors have already reported explosive radiation during the formation process of the naked singularity which occurs in the collapse of an inhomogeneous dust ball from the initial density profile which is a C^∞ function [24]. In this paper, we present the details of the calculations in the above paper and examine power, energy, and spectrum of that radiation process.

This paper is organized as follows. In Sec. II, we will recall the least of quantum particle creation by a collapsing ball based on the geometrical optics approximation. In Sec. III, we present the background solution of spacetime which describes the collapse of an inhomogeneous dust ball. In Sec. IV, we present numerical results of power and energy due to the quantum particle creation and give some physical discussions. In Sec. V, we determine the spectrum of the radiation which is important not only astrophysically but also in estimating the validity of the geometrical optics approximation. In Sec. VI, we analytically examine null geodesics and redshifts in this spacetime and thereby understand some features of the numerical results. In Sec. VII, we estimate the validity of the geometrical optics approximation. In Sec. VIII, some implications of the emission from the forming naked singularity are discussed. In Sec. IX, we conclude the paper. We use the units in which $G = c = \hbar = 1$ unless explicitly stated. We follow the sign conventions of Misner, Thorne, and Wheeler [25].

II. PARTICLE CREATION BY A COLLAPSING BALL

We consider both minimally and conformally coupled massless scalar fields in a four-dimensional spacetime which is spherically symmetric and asymptotically flat. Let T, R, θ, ϕ denote the usual quasi-Minkowskian time and spherical coordinates, which are asymptotically related to null coordinates u and v by $u \approx T - R$ and $v \approx T + R$. An incoming

null ray $v = \text{const}$, originating on \mathfrak{S}^- , propagates through the geometry becoming an outgoing null ray $u = \text{const}$, and arriving on \mathfrak{S}^+ at a value $u = F(v)$. Conversely, we can trace a null ray from u on \mathfrak{S}^+ to $v = G(u)$ on \mathfrak{S}^- , where G is the inverse of F . Here, we assume that the geometrical optics approximation is valid. The validity of this approximation will be discussed later. The geometrical optics approximation implies that the trajectories of the null rays give a surface of the constant phase. Then, in the asymptotic region, the mode function which contains an ingoing mode of the standard form on \mathfrak{S}^- is the following:

$$u_{\omega lm}^{in} \approx \frac{1}{\sqrt{4\pi\omega R}}(e^{-i\omega v} - e^{-i\omega G(u)})Y_{lm}(\theta, \phi), \quad (2.1)$$

where we have imposed the reflection symmetry condition at the center. On the other hand, in the asymptotic region, the mode function which contains an outgoing mode of the standard form on \mathfrak{S}^+ is the following:

$$u_{\omega lm}^{out} \approx \frac{1}{\sqrt{4\pi\omega R}}(e^{-i\omega F(v)} - e^{-i\omega u})Y_{lm}(\theta, \phi). \quad (2.2)$$

Note that in the above we have normalized the mode functions as

$$(u_{\omega lm}, u_{\omega' l' m'}) = \delta(\omega - \omega')\delta_{ll'}\delta_{mm'}, \quad (2.3)$$

where the inner product is defined by integration on the spacelike hypersurface Σ as

$$(\psi, \chi) = -i \int_{\Sigma} (\psi \chi_{,\mu}^* - \psi_{,\mu} \chi^*) \sqrt{g_{\Sigma}} d\Sigma^{\mu}. \quad (2.4)$$

Using the above mode functions we can express the scalar field ϕ as

$$\phi = \sum_{l,m} \int d\omega' (\mathbf{a}_{\omega' lm}^{in} u_{\omega' lm}^{in} + \mathbf{a}_{\omega' lm}^{in\dagger} u_{\omega' lm}^{in*}), \quad (2.5)$$

$$\phi = \sum_{l,m} \int d\omega' (\mathbf{a}_{\omega' lm}^{out} u_{\omega' lm}^{out} + \mathbf{a}_{\omega' lm}^{out\dagger} u_{\omega' lm}^{out*}). \quad (2.6)$$

According to the usual procedure of canonical quantization, we obtain the following commutation relations

$$[\mathbf{a}_{\omega lm}^{in}, \mathbf{a}_{\omega' l' m'}^{in\dagger}] = \delta(\omega - \omega')\delta_{ll'}\delta_{mm'}, \quad (2.7)$$

$$[\mathbf{a}_{\omega lm}^{out}, \mathbf{a}_{\omega' l' m'}^{out\dagger}] = \delta(\omega - \omega')\delta_{ll'}\delta_{mm'}, \quad (2.8)$$

where it is noted that the Lagrangian in the Minkowski spacetime is common for both minimally and conformally coupled scalar fields. Here, $\mathbf{a}_{\omega lm}^{in}$ and $\mathbf{a}_{\omega lm}^{out}$ are interpreted as annihilation operators corresponding to in and out modes, respectively. Then we set the initial quantum state to in vacuum, i.e.,

$$\mathbf{a}_{\omega lm}^{in}|0\rangle = 0. \quad (2.9)$$

The power for fixed l and m is given by estimating the expectation value of the stress-energy tensor through the point-splitting regularization in a flat spacetime as [16]

$$P_{lm} \equiv \int \langle T_T^R \rangle R^2 d\Omega = \frac{1}{24\pi} \left[\frac{3}{2} \left(\frac{G''}{G'} \right)^2 - \frac{G'''}{G'} \right] = \frac{1}{48\pi} \left(\frac{G''}{G'} \right)^2 - \frac{1}{24\pi} \left(\frac{G''}{G'} \right)' \quad (2.10)$$

for a minimally coupled scalar field, and

$$\hat{P}_{lm} \equiv \int \langle \hat{T}_T^R \rangle R^2 d\Omega = \frac{1}{48\pi} \left(\frac{G''}{G'} \right)^2 \quad (2.11)$$

for a conformally coupled scalar field. It implies that the power depends on the method of coupling of the scalar field with gravity. However, if

$$\left. \frac{G''}{G'} \right|_a = \left. \frac{G''}{G'} \right|_b \quad (2.12)$$

holds, the radiated energy from $u = a$ to $u = b$ of a minimally coupled field

$$E_{lm} \equiv \int_a^b P_{lm} du \quad (2.13)$$

and that of a conformally coupled field

$$\hat{E}_{lm} \equiv \int_a^b \hat{P}_{lm} du \quad (2.14)$$

coincide exactly. The total power is given by summation of all (l, m) . The simple summation diverges. This is because we have neglected the back scattering effect by the curvature potential, which will reduce the radiated flux considerably for larger l . Therefore we should recognize that the above expressions of the power, Eqs. (2.10) and (2.11), are a good approximation only for smaller l . Hereafter we omit the suffix l and m .

The spectrum of radiation is derived from the Bogoliubov coefficients which relate the in and out modes given by [26]

$$\alpha_{\omega'\omega} = (u_{\omega'}^{in}, u_{\omega}^{out}) = \frac{1}{2\pi} \sqrt{\frac{\omega'}{\omega}} \int_{-\infty}^{\infty} dv e^{i\omega F(v) - i\omega'v}, \quad (2.15)$$

$$\beta_{\omega'\omega} = -(u_{\omega'}^{in}, u_{\omega}^{out*}) = -\frac{1}{2\pi} \sqrt{\frac{\omega'}{\omega}} \int_{-\infty}^{\infty} dv e^{-i\omega F(v) - i\omega'v}. \quad (2.16)$$

From the above equations, we find the following useful relation:

$$\beta_{\omega'\omega} = -i\alpha_{\omega'(-\omega)}. \quad (2.17)$$

The Bogoliubov coefficients satisfy the following relations:

$$\int_0^{\infty} d\tilde{\omega} (\alpha_{\tilde{\omega}\omega} \alpha_{\tilde{\omega}\omega'}^* - \beta_{\tilde{\omega}\omega} \beta_{\tilde{\omega}\omega'}^*) = \delta(\omega - \omega'), \quad (2.18)$$

$$\int_0^{\infty} d\tilde{\omega} (\alpha_{\tilde{\omega}\omega} \beta_{\tilde{\omega}\omega'} - \beta_{\tilde{\omega}\omega} \alpha_{\tilde{\omega}\omega'}) = 0. \quad (2.19)$$

The expectation value $N(\omega)$ of the particle number of frequency ω on \mathfrak{S}^+ is obtained by

$$N(\omega) = \int_0^{\infty} d\omega' |\beta_{\omega'\omega}|^2. \quad (2.20)$$

It is noted that these results are free of ambiguity coming from local curvature because the regularization is done in a flat spacetime.

III. LEMAITRE-TOLMAN-BONDI SOLUTION

The spherically symmetric collapse of a dust fluid is exactly solved [27,28]. The solution is called the Lemaître-Tolman-Bondi (LTB) solution. The metric is given by

$$ds^2 = -dt^2 + \frac{(R,r)^2(t,r)}{1+f(r)} dr^2 + R^2(t,r)(d\theta^2 + \sin^2\theta d\phi^2) \quad (3.1)$$

in the synchronous comoving coordinates. The matter field is given by

$$T^{\mu\nu} = \epsilon u^\mu u^\nu, \quad (3.2)$$

$$\epsilon = \frac{F'(r)}{8\pi R^2 R_{,r}}. \quad (3.3)$$

$F(r)$ and $f(r)$ are arbitrary functions. $F(r)$ is the mass function, which is twice the Misner-Sharp mass. $f(r)$ is the energy function. The areal radius R satisfies the following equation:

$$(R,t)^2 = \frac{F(r)}{R} + f(r). \quad (3.4)$$

Equation (3.4) is integrated to the following form

$$t - t_s(r) = -\sqrt{\frac{R^3}{F}} g\left(-\frac{fR}{F}\right), \quad (3.5)$$

where $g(y)$ is a positive function given by

$$g(y) = \begin{cases} \frac{\text{Arcsin}\sqrt{y}}{y^{3/2}} - \frac{\sqrt{1-y}}{y} & \text{for } 0 < y \leq 1, \\ \frac{2}{3} & \text{for } y = 0, \\ \frac{-\text{Arcsinh}\sqrt{-y}}{(-y)^{3/2}} - \frac{\sqrt{1-y}}{y} & \text{for } y < 0, \end{cases} \quad (3.6)$$

$t_s(r)$ is a constant of integration, and the sign is chosen so that the collapsing phase is relevant. Note that the metric has physical meaning only on $0 \leq r$ and $t < t_s(r)$. We rescale the radial coordinate r as follows

$$R(0, r) = r. \quad (3.7)$$

From Eq. (3.3), if we require that the initial density profile at $t = 0$ is a C^∞ function with respect to the local Cartesian coordinates, $F(r)$ should be expanded around $r = 0$ as

$$F(r) = F_3 r^3 + F_5 r^5 + F_7 r^7 + \dots, \quad (3.8)$$

where we assume that F_3 is positive. Then, $t_s(r)$ is given by

$$t_s(r) = \sqrt{\frac{r^3}{F}} g\left(-\frac{fr}{F}\right). \quad (3.9)$$

We can easily find that the time of the occurrence of shell-focusing singularity is given by $t_s(r)$, while the time of the occurrence of apparent horizon is given by

$$t_{ah}(r) = t_s(r) - Fg(-f). \quad (3.10)$$

Hereafter we assume marginally bound collapse ($f = 0$) for simplicity.

At an arbitrary radius r , the LTB spacetime can be matched with the Schwarzschild spacetime

$$ds^2 = -\left(1 - \frac{2M}{R}\right) dT^2 + \left(1 - \frac{2M}{R}\right)^{-1} dR^2 + R^2(d\theta^2 + \sin^2\theta d\phi^2). \quad (3.11)$$

The matching conditions with the Schwarzschild spacetime are obtained by requiring that the surface moves on the timelike geodesic and that the three metric on the timelike hypersurface should be continuous. The result is

$$T = t - \frac{2r^{3/2}}{3\sqrt{2M}} - 2\sqrt{2MR} + 2M \ln \frac{\sqrt{R} + \sqrt{2M}}{\sqrt{R} - \sqrt{2M}}, \quad (3.12)$$

$$R = R(t, r), \quad (3.13)$$

$$M = \frac{F(r)}{2}, \quad (3.14)$$

at the surface $r = r_{sf}$. The retarded time u and the advanced time v in the Schwarzschild spacetime are defined by

$$u = T - R - 2M \ln \frac{R - 2M}{2M}, \quad (3.15)$$

$$v = T + R + 2M \ln \frac{R - 2M}{2M}. \quad (3.16)$$

For the case of marginally bound collapse, R is given by

$$R = r \left(1 - \frac{3}{2} \sqrt{\frac{F}{r^3}} t \right)^{2/3}. \quad (3.17)$$

The occurrence of singularity is at the time

$$t_s(r) = \frac{2}{3} \sqrt{\frac{r^3}{F}}. \quad (3.18)$$

Each mass shell is trapped at the time

$$t_{ah}(r) = \frac{2}{3} \sqrt{\frac{r^3}{F}} - \frac{2}{3} F. \quad (3.19)$$

We denote the time of the occurrence of the singularity at the center as $t_0 \equiv t_s(0)$.

Detailed analysis on the occurrence of naked shell-focusing singularity has been done in [1–4,29–31]. Here we present one of the results. If we assume marginally bound collapse and assume the initial density profile expressed by Eq. (3.8), then the central shell-focusing singularity is naked if and only if F_5 is negative. The singularity satisfies not the strong curvature condition (SCC) defined by Tipler [32] but only the limiting focusing condition (LFC) defined by Królak [33] for radial null geodesics which terminate at the singularity. On the other hand, the singularity satisfies both LFC and SCC for radial timelike geodesics [21].

IV. POWER AND ENERGY

A. Globally naked singularity

We can find the function G or F by solving the trajectories of outgoing and ingoing null rays in the dust cloud and determining the retarded time u and the advanced time v through Eqs. (3.15) and (3.16) at the time when the outgoing and ingoing null rays reach the surface boundary, respectively. The trajectories of null rays in the dust cloud are given by the following ordinary differential equation:

$$\frac{dt}{dr} = \pm R_{,r}, \quad (4.1)$$

where the upper and lower signs denote outgoing and ingoing null rays, respectively.

We have solved the ordinary differential equation (4.1) numerically. We have used the Runge-Kutta method of the fourth order. We have executed the quadruple precision calculations.

We choose the mass function as

$$F(r) = F_3 r^3 + F_5 r^5. \quad (4.2)$$

We find that the central singularity is globally naked for very small r_{sf} if we fix the values of F_3 and F_5 . Although we have calculated several models, we only display the numerical results for the model with $F_3 = 1$, $F_5 = -2$ and $r_{sf} = 0.02$ in an arbitrary unit because the features are the same if there exists globally naked singularity in the model. The total gravitational mass M is given by $M = 3.9968 \times 10^{-6}$ for this model. See Fig. 1 for trajectories of null geodesics. We also indicate the location of the singularity, the apparent horizon, and the Cauchy horizon in this figure.

See Fig. 2. In Fig. 2(a), the relation between u and v , i.e., the function $G(u)$ is shown, where u_0 (v_0) is defined as the retarded (advanced) time of the earliest light ray which originates from (terminates at) the singularity. In Fig. 2(b), the first derivative $G'(u)$ is shown. This implies that $G'(u)$ does not diverge but converges to some positive constant A with $0 < A < 1$. In Fig. 2(c), it is found that the second derivative $G''(u)$ does diverge as $u \rightarrow u_0$. This figure shows that the behaviors of the growth of $G''(u)$ are different from each other during early times ($10^{-4} \lesssim u_0 - u$) and during late times ($0 < u_0 - u \lesssim 10^{-4}$). During early times, the dependence on u is written as

$$G'' \propto -(-u)^{-2}, \quad (4.3)$$

while, during late times, the dependence is written as

$$G'' \propto -(u_0 - u)^{-1/2}. \quad (4.4)$$

Here we determine the magnitude of the power by physical discussions. We assume that the particle creation during early times is due to the collapse of the dust cloud as a whole while that during late times is due to the growth of the central curvature. Then, we consider a constant of proportion which will appear in Eqs. (4.3) and (4.4). First we should note that the coefficient must be written by initial data because it must not depend on time. Next we should note that we can identify any $t = \text{const} < t_0$ hypersurface with the initial hypersurface. Since the constant of proportion directly enters the expression of the power which is physically meaningful, the coefficient must be independent of the choice of an initial slice. On the other hand, Eqs. (4.3) and (4.4) demand a dimensionful constant of proportion. For early times, the only possible quantity is the gravitational mass M of the dust cloud. On the other hand, for late times, as derived in Appendix A, the only possible quantity is (t_0^7/l_0^6) , where t_0 is given by

$$t_0 = \frac{2}{3}F_3^{-1/2}, \quad (4.5)$$

and l_0 denotes the scale of inhomogeneity defined as

$$l_0 \equiv \left(\frac{-F_5}{F_3} \right)^{-1/2}. \quad (4.6)$$

Thus we can determine the coefficient except for a numerical factor as

$$G'' \approx -f_e M (-u)^{-2}, \quad (4.7)$$

for early times, while the dependence is written as

$$G'' \approx -f_l A \left(\frac{t_0^7}{l_0^6} \right)^{-1/2} (u_0 - u)^{-1/2}, \quad (4.8)$$

for late times, where f_e and f_l are dimensionless positive constants of order unity. It implies that there is a characteristic frequency of singularity which is defined as

$$\omega_s \equiv \frac{l_0^6}{t_0^7}. \quad (4.9)$$

The early time behavior derived above is good for $-u \gg M$, while the late time behavior is good for $0 < u_0 - u \ll \omega_s^{-1}$. The turning point from the early time behavior to the late time behavior is roughly estimated as

$$u_0 - u \approx (M\omega_s)^{2/3}\omega_s^{-1} = (M\omega_s)^{-1/3}M. \quad (4.10)$$

Here we define the turning point frequency ω_{tp} as

$$\omega_{tp} \equiv (M\omega_s)^{-2/3}\omega_s = (M\omega_s)^{1/3}M^{-1}. \quad (4.11)$$

The above estimates show a good agreement with the numerical results.

Since G'' and therefore G''' diverge as $u \rightarrow u_0$, the power of radiation diverges for both minimally and conformally coupled scalar fields. For this model, we have numerically calculated the power of radiation by Eqs. (2.10) and (2.11). The results are displayed in Fig. 3.

Based on the above physical discussions, we can obtain the formula for the power by the particle creation using Eqs. (2.10) and (2.11). As seen in Fig. 2(b), we find

$$G' \approx 1 \quad (4.12)$$

during early times, and

$$G' \approx A, \quad (4.13)$$

during late times. Then, the power during early times is obtained as

$$P \approx \frac{1}{12\pi} f_e M (-u)^{-3}, \quad (4.14)$$

$$\hat{P} \approx \frac{1}{48\pi} f_e^2 M^2 (-u)^{-4}. \quad (4.15)$$

The power during late times is obtained as

$$P \approx \frac{1}{48\pi} f_l \omega_s^{1/2} (u_0 - u)^{-3/2}, \quad (4.16)$$

$$\hat{P} \approx \frac{1}{48\pi} f_l^2 \omega_s (u_0 - u)^{-1}. \quad (4.17)$$

Therefore, the power diverges to positive infinity for both minimally and conformally coupled scalar fields as $u \rightarrow u_0$. The radiated energy is estimated by integrating the power with time. During late times, the radiated energy is estimated as

$$E \approx \frac{1}{24\pi} f_l \omega_s^{1/2} (u_0 - u)^{-1/2}, \quad (4.18)$$

$$\hat{E} \approx \frac{1}{48\pi} f_l^2 \omega_s \ln \frac{(M\omega_s)^{2/3}}{\omega_s(u_0 - u)}. \quad (4.19)$$

Therefore, the total radiated energy diverges to positive infinity for both minimally and conformally coupled scalar fields as $u \rightarrow u_0$. However, in realistic situations, we may assume that the naked singularity formation is prevented by some mechanism and that the quantum particle creation is ceased at the time $u_0 - u \approx \Delta t$. In other words, G''/G' tends to vanish for $u_0 - u \lesssim \Delta t$. In such situations, the total divergence term in the expression of the power of a minimally coupled scalar field gives no contribution to the total radiated energy. Therefore, the total energy for a minimally coupled scalar field and that for a conformally coupled one coincide exactly, i.e.,

$$E = \hat{E} \approx \frac{1}{48\pi} f_l^2 \omega_s \ln \frac{(M\omega_s)^{2/3}}{\omega_s \Delta t}. \quad (4.20)$$

The relation of Δt and the maximum central energy density ϵ_c^{max} of the dust cloud at that time is given by

$$\epsilon_c^{max} \sim (\Delta t)^{-2}. \quad (4.21)$$

From the above numerical results and physical discussions, we obtain the following formula for the function $G(u)$ or $F(v)$:

$$G(u) \approx u + f_e M \ln(-u) \quad (4.22)$$

or

$$F(v) \approx v - f_e M \ln(-v) \quad (4.23)$$

for early times, and

$$G(u) \approx A(u - u_0) - \frac{4}{3} A f_l \omega_s^{1/2} (u_0 - u)^{3/2} + v_0 \quad (4.24)$$

or

$$F(v) \approx A^{-1}(v - v_0) + \frac{4}{3} f_l \omega_s^{1/2} [A^{-1}(v_0 - v)]^{3/2} + u_0 \quad (4.25)$$

for late times.

B. Black hole

For comparison and for a test of the numerical code, we have also calculated the function G for the Oppenheimer-Snyder collapse. The model is given by setting $F_3 = 1$, $F_5 = 0$, and $r_{sf} = 0.2$ ($M = 4 \times 10^{-3}$) in Eq. (4.2) in an arbitrary unit.

The final fate of the Oppenheimer-Snyder collapse is a spacelike singularity covered by the event horizon. Then it is expected that radiation during the collapse tends to Hawking radiation as $u \rightarrow \infty$. In reality, this is true. See Fig. 4 in which trajectories of null geodesics are displayed. We can see that the event horizon covers the singularity. See Fig. 5 for the behavior of the functions $G(u)$, $G'(u)$, and $G''(u)$. During early times, the behavior of $G(u)$ is basically the same as that of the globally naked singularity, i.e., $G(u)$ is written as

$$G(u) \approx u + f_e M \ln(-u). \quad (4.26)$$

This is very reasonable because the behavior during early times will be independent of details of the density profile within the dust cloud. During late times, G is written as follows

$$G(u) \approx -\text{const} \times \exp\left(\frac{-u}{4M}\right) + v_h, \quad (4.27)$$

where an ingoing null ray with v_h is reflected to the outgoing null ray which is on the event horizon. This relation will be derived later.

The power of radiation has been calculated numerically. During early times, the power is the same as that for globally naked singularity. The results are shown in Fig. 6. On the other hand, from Eq. (4.27), we can estimate the power and the radiated energy during late times as

$$P = \hat{P} \approx \frac{1}{768\pi M^2}, \quad (4.28)$$

$$E = \hat{E} \approx \frac{1}{768\pi M^2} u. \quad (4.29)$$

The numerical results show a good agreement with these analytic results. The numerical result for the power of radiation in this model has reproduced that of the Hawking radiation (4.28) by a black hole within $\sim 0.01\%$ accuracy.

We should also note that the late time radiation during the LTB collapse with the locally naked singularity is the same as that of the Oppenheimer-Snyder collapse. This is because a distant observer cannot see the locally naked singularity.

V. SPECTRUM

A. Total spectrum

Now that we have obtained the function $F(v)$, we can calculate the spectrum of radiation by Eqs. (2.15), (2.16), and (2.20). Some analytic expressions for the Bogoliubov coefficients are obtained in Appendix B. In order to determine the spectrum numerically, we introduce the Gaussian window function in the Fourier transformation as usual. That is, in place of Eqs. (2.15) and (2.16), we have calculated the Bogoliubov coefficients

$$\tilde{\alpha}_{\omega'\omega} \equiv \frac{1}{2\pi} \sqrt{\frac{\omega'}{\omega}} \int_{-\infty}^{\infty} dv e^{i\omega F(v) - i\omega'v} \frac{1}{\sqrt{4\pi\Sigma}} \exp\left[-\left(\frac{F(v) - u_c}{\Sigma}\right)^2\right], \quad (5.1)$$

$$\tilde{\beta}_{\omega'\omega} \equiv -\frac{1}{2\pi} \sqrt{\frac{\omega'}{\omega}} \int_{-\infty}^{\infty} dv e^{-i\omega F(v) - i\omega'v} \frac{1}{\sqrt{4\pi\Sigma}} \exp\left[-\left(\frac{F(v) - u_c}{\Sigma}\right)^2\right], \quad (5.2)$$

where u_c and Σ are the center and the width of the Gaussian window function, respectively. Since the wave packet

$$\frac{1}{\sqrt{4\pi\Sigma}} e^{i\omega u} \exp\left[-\left(\frac{u - u_c}{\Sigma}\right)^2\right] \quad (5.3)$$

has the frequency band width $\Delta\omega \sim 2/\Sigma$, we can obtain the number of particles per unit frequency band as

$$\frac{dN}{d\omega} \sim \frac{\Sigma}{2} \left[\frac{\int_0^\infty d\omega' |\tilde{\alpha}_{\omega'\omega}|^2}{\int_0^\infty d\omega' |\tilde{\beta}_{\omega'\omega}|^2} - 1 \right]^{-1}, \quad (5.4)$$

where we have again assumed that the geometrical optics approximation is valid.

Although we could use the calculated data for the function $F(v)$, we have used the analytic formula which have been derived based on the numerical results for convenience of retaining accuracy. Since the diverging power is associated with the late time behavior, we concentrate on the late time radiation. In order to obtain the total spectrum, we extrapolate the function F linearly as

$$F(v) = \begin{cases} A^{-1}(v - v_0) + u_0 & (v_0 < v), \\ A^{-1}(v - v_0) + \frac{4}{3}f_l\omega_s^{1/2}[A^{-1}(v_0 - v)]^{3/2} + u_0 & (v_1 < v \leq v_0), \end{cases} \quad (5.5)$$

where v_1 is given by

$$v_0 - v_1 \equiv \left[\frac{1}{2}(1 - A)f_l^{-1} \right]^2 A\omega_s^{-1}. \quad (5.6)$$

We should note that Eq. (5.5) can be used for $u_0 - u \lesssim \omega_{tp}^{-1}$. Later we will show that $\omega_{tp} \gtrsim \omega_s$ for $r_{sf} \ll l_0$. In fact, it turns out that we only have to pay attention to the spectrum above ω_{tp} . We have chosen $u_c = u_0$ and Σ to be rather smaller than $u_0 - u_1$ with $u_1 = F(v_1)$, for the contribution dominantly comes from $u \approx u_0$. We should note that there is no radiation for $u > u_0$ in this extrapolation. We could adopt another extrapolation, for example, an extrapolation such that $F(v) - u_0$ is antisymmetric with respect to $v = v_0$, i.e.,

$$F(v) = \begin{cases} A^{-1}(v - v_0) - \frac{4}{3}f_l\omega_s^{1/2}[A^{-1}(v - v_0)]^{3/2} + u_0 & (v_0 < v < 2v_0 - v_1), \\ A^{-1}(v - v_0) + \frac{4}{3}f_l\omega_s^{1/2}[A^{-1}(v_0 - v)]^{3/2} + u_0 & (v_1 < v \leq v_0), \end{cases} \quad (5.7)$$

This antisymmetric extrapolation turns out to only double the amplitude of the spectrum through the linear extrapolation (5.5). Therefore, we only present the spectrum through the linear extrapolation. Because the second derivative of F is diverging as $v \rightarrow v_0$, we can only require that the first derivative of F should be continuous at $v = v_0$. If we allow discontinuity of the first derivative, radiation due to this discontinuity dominates the radiated energy flux, which is out of concern in this paper.

The obtained spectrum is shown in Fig. 7. The parameters are fixed as $A = 0.8$ and $f_l = 1$. We should note that the contribution to the total radiated energy mainly comes from $\omega \gtrsim \omega_{tp}$. In this figure, we find

$$\omega \frac{dN}{d\omega} \propto \omega^{-1}. \quad (5.8)$$

Therefore, the total energy, which will be obtained by

$$E = \int_0^\infty d\omega \omega \frac{dN}{d\omega}, \quad (5.9)$$

is logarithmically divergent, which is consistent with the diverging radiated energy obtained in Sec. IV based on the point-splitting regularization.

For $u > u_0$, if we respect the causal structure of the background LTB spacetime, in which the naked singularity is ingoing null, an ingoing null ray never changes into an outgoing null ray. It is obvious that the geometrical optics approximation will be no longer valid after the formation of the naked singularity. Therefore, we need to determine mode functions by other methods than the geometrical optics approximation. On the other hand, we have seen that the unbounded power and energy are radiated before the occurrence of the naked singularity. Then, we could expect that naked singularity formation will be prevented for some physical mechanism. For example, the back reaction of the quantum effect might prevent naked singularity formation. In fact, the LTB spacetime is only an approximation of realistic gravitational collapse. Violation of spherical symmetry, rotational support, hardening of an equation of state, ignition of nuclear burning, quantum gravity, and so on might make the approximation by the LTB spacetime no longer valid in the final stage of the realistic collapse. From the above discussions, the causal structure of the LTB spacetime after naked singularity formation cannot be taken seriously.

B. Momentary spectrum

It is important in estimating the validity of the geometrical optics approximation to examine which frequency band dominates the power at some moment. For this purpose, we determine the momentary spectrum by wavelet analysis. We use Gabor's mother wavelet[§] in place of e^{ix} because it has a very clear physical meaning as a Gaussian wave packet. We consider Gabor's mother wavelet

[§]The Gabor wavelet is sometimes referred to as the Morlet wavelet. Strictly speaking, Gabor's mother wavelet does not become a basis function. However, it is known that this wavelet with an appropriate value of σ is useful in finding the frequency of the signal.

$$\psi(x) = \frac{1}{\sqrt{4\pi\sigma}} e^{ix} e^{-x^2/\sigma^2}, \quad (5.10)$$

where we have set $\sigma = 8$. The result below is not so sensitive to the value of σ . We can obtain the Bogoliubov coefficients as

$$\bar{\alpha}_{\omega'\omega} \equiv \frac{1}{2\pi} \sqrt{\frac{\omega'}{\omega}} \int_{-\infty}^{\infty} dv \psi[\omega(F(v) - u)] e^{-i\omega'v}, \quad (5.11)$$

$$\bar{\beta}_{\omega'\omega} \equiv -\frac{1}{2\pi} \sqrt{\frac{\omega'}{\omega}} \int_{-\infty}^{\infty} dv \psi^*[\omega(F(v) - u)] e^{-i\omega'v}, \quad (5.12)$$

where u is chosen to be the observation time. Because the Gabor wavelet occupies area $\Delta\omega\Delta u \sim 2$ in the phase space (u, ω) , the momentary number spectrum is given by

$$\frac{dN}{d\omega du} \sim \frac{1}{2} \Gamma_{\omega} \left[\frac{\int_0^{\infty} d\omega' |\bar{\alpha}_{\omega'\omega}|^2}{\int_0^{\infty} d\omega' |\bar{\beta}_{\omega'\omega}|^2} - 1 \right]^{-1}, \quad (5.13)$$

where Γ_{ω} is the transmission coefficient, which we tentatively assume $\Gamma_{\omega} = 1$.

We have calculated numerically the momentary spectrum. The result is shown in Fig. 8. This figure displays the contribution of each logarithmic bin of frequency to the power at the moment. The parameters are fixed as $A = 0.8$ and $f_l = 1$. We have chosen the time of observation $u = 10^{-6}\omega_s^{-1}$. The shape of the spectrum looks somewhat like the thermal one but the normalization of the spectrum is different. In this figure, it is found that the contribution to the power is dominated by the frequency $\omega \sim 2\pi(u_0 - u)^{-1}$. For a conformally coupled scalar field, the integration of the obtained $\omega dN/(d\omega du)$ with ω recovers the power derived by the point-splitting regularization except for a numerical factor of order unity, i.e.,

$$\int d\omega \omega \frac{dN}{d\omega du} \sim \hat{P}. \quad (5.14)$$

For a minimally coupled scalar field, such a correspondence cannot be seen. For a conformally coupled scalar field, since the power is mainly transported by particles with a frequency of about $2\pi(u_0 - u)^{-1}$, the radiated number of particles per unit time is constant, being roughly estimated from Eq. (4.17) as

$$\frac{dN}{du} \sim \omega_s. \quad (5.15)$$

From this equation, we can roughly estimate as

$$\omega \frac{dN}{d\omega} \sim \frac{\omega_s}{\omega}, \quad (5.16)$$

which recovers the total spectrum except for a numerical factor. From the above analysis, we can conclude that the total divergence term in the expression for the power of a minimally coupled scalar field has nothing to do with the observed particle number.

VI. NULL GEODESICS AND REDSHIFTS IN LTB SPACETIME

A. Assumption

Here we analytically examine null geodesics and redshifts in the LTB spacetime and derive some useful results to comprehend the problem. We assume the function $F(r)$ of the form (3.8) with $F_3 > 0$ and $F_5 < 0$. From Eq. (3.17), R and $R_{,r}$ are written for $r/l_0 \ll 1$ as

$$R \approx r \left[\left(\frac{-\eta}{t_0} \right) \left\{ 1 - \frac{1}{2} \left(\frac{r}{l_0} \right)^2 \right\} + \frac{1}{2} \left(\frac{r}{l_0} \right)^2 \right]^{2/3}, \quad (6.1)$$

$$R_{,r} \approx \left[\left(\frac{-\eta}{t_0} \right) \left\{ 1 - \frac{7}{6} \left(\frac{r}{l_0} \right)^2 \right\} + \frac{7}{6} \left(\frac{r}{l_0} \right)^2 \right] \left[\left(\frac{-\eta}{t_0} \right) \left\{ 1 - \frac{1}{2} \left(\frac{r}{l_0} \right)^2 \right\} + \frac{1}{2} \left(\frac{r}{l_0} \right)^2 \right]^{-1/3}, \quad (6.2)$$

where η is defined as

$$\eta \equiv t - t_0. \quad (6.3)$$

Moreover, $\eta_s(r) \equiv t_s(r) - t_0$ and $\eta_{ah}(r) \equiv t_{ah}(r) - t_0$ are approximated for $r/l_0 \ll 1$ as

$$\frac{\eta_s(r)}{t_0} \approx \frac{1}{2} \left(\frac{r}{l_0} \right)^2, \quad (6.4)$$

$$\frac{\eta_{ah}(r)}{t_0} \approx \frac{1}{2} \left(\frac{r}{l_0} \right)^2 - \left(\frac{2}{3} \right)^3 \left(\frac{l_0}{t_0} \right)^3 \left(\frac{r}{l_0} \right)^3. \quad (6.5)$$

For simplicity, we assume

$$\frac{r_{sf}}{l_0} \ll 1. \quad (6.6)$$

This implies that we can safely expand in powers of r/l_0 and take the leading-order term *in the whole of the cloud*.

B. Trajectories

First we consider the region where

$$\left(\frac{r}{l_0} \right)^2 \ll \left| \frac{\eta}{t_0} \right| \quad (6.7)$$

is satisfied. This region is approximately recognized as the Friedmann universe. From Eq. (6.4), it is found that this condition can be satisfied only for $\eta < 0$. In this case, $R_{,r}$ is approximated as

$$R_{,r} \approx \left(\frac{-\eta}{t_0} \right)^{2/3}. \quad (6.8)$$

The ordinary differential equation (4.1) can be easily integrated to

$$\left(\frac{-\eta}{t_0} \right)^{1/3} \approx \mp \frac{1}{3} \left(\frac{l_0}{t_0} \right) \left(\frac{r}{l_0} \right) + C_{A\pm}, \quad (6.9)$$

where $C_{A\pm}$ is a constant of integration. It is easily found that each null ray can be drawn by a parallel transport of the curve with $C_{A\pm} = 0$ along the r -axis direction.

Next we consider the region where

$$\left(\frac{r}{l_0} \right)^2 \gg \left| \frac{\eta}{t_0} \right| \quad (6.10)$$

is satisfied. This region is not at all approximated by the Friedmann universe. In this case, $R_{,r}$ is approximated as

$$R_{,r} \approx \frac{7}{2^{2/3}3} \left(\frac{r}{l_0} \right)^{4/3}. \quad (6.11)$$

Then Eq. (4.1) is integrated to

$$\frac{\eta}{t_0} \approx \pm 2^{-2/3} \left(\frac{l_0}{t_0} \right) \left(\frac{r}{l_0} \right)^{7/3} - C_{B\pm}, \quad (6.12)$$

where $C_{B\pm}$ is a constant of integration. It is easily found that each null ray can be drawn by a parallel transport of the curve with $C_{B\pm} = 0$ along the η -axis direction.

See Fig. 9, which illustrates the spacetime around $(\eta, r) = (0, 0)$. Condition (6.7) is satisfied in region A , while condition (6.10) is satisfied in region B . The boundary of regions A and B will be described by

$$\frac{-\eta}{t_0} = \gamma \left(\frac{r}{l_0} \right)^2, \quad (6.13)$$

where γ is a constant of order unity. We denote this boundary curve as C . It may be kept in mind that this treatment is rather simple. However, we believe that the present approximation, where we divide the spacetime into two regions, will be enough to comprehend the essence of the problem.

Then, we concentrate on the behavior of null geodesics around the naked singularity. See Fig. 9 for the trajectory of null geodesics. From the regular center $\eta < 0$ and $r = 0$, the outgoing null ray runs region A which is described by the upper sign of Eq. (6.9) with $C_{A+} > 0$. Then this null ray goes through boundary C . After that the null ray goes into region B and the trajectory is described by the upper sign of Eq. (6.12) with $C_{B+} > 0$. Since all null rays with $C_{B+} > 0$ in region B emanate from the regular center, the outgoing null geodesic with $C_{B+} = 0$ in region B generates the Cauchy horizon. In other words, it is the earliest outgoing null ray from the singularity at $r = 0$. We denote this outgoing null geodesic as n_{0+} . There are infinitely many outgoing null geodesics later than n_{0+} which emanates from the naked singularity at $r = 0$. In fact, these null geodesics form one parameter family. These null rays cannot asymptote to n_{0+} as $r \rightarrow 0$ because these null rays are obtained by parallel transport of n_{0+} in the η -axis direction in region B . Instead, the location of the apparent horizon $\eta = \eta_{ah}(r)$ is an asymptote of these outgoing null rays in approaching the naked singularity.

On the other hand, it is clear that the ingoing null ray with $C_{B-} = 0$ terminates at the singularity $r = 0$. We denote this ingoing null ray as n_{0-} . For small positive C_{B-} , the ingoing null ray in region B crosses to boundary C and the null ray becomes described by the lower sign of Eq. (6.9) with $C_{A-} > 0$, and then terminates at the regular center. For small negative C_{B-} , the ingoing null ray in region B terminates at the spacelike singularity $r > 0$.

C. Condition for globally naked singularity

If n_{0+} reach \mathfrak{S}^+ , then the singularity is globally naked, otherwise the singularity is locally naked. Noting that the intersection of the apparent horizon with the cloud surface is on the event horizon, we find that the condition for the singularity to be globally naked is given by

$$\left[\left(\frac{l_0}{t_0} \right) \left(\frac{r_{sf}}{l_0} \right)^{1/3} \right]^{-1} - \frac{16}{27} \left[\left(\frac{l_0}{t_0} \right) \left(\frac{r_{sf}}{l_0} \right)^{1/3} \right]^2 \gtrsim 2^{1/3}. \quad (6.14)$$

Since $x^{-1} - (16/27)x^2$ is a decreasing function of $x > 0$, we can find the condition for the singularity to be globally naked as

$$\frac{r_{sf}}{l_0} \lesssim 0.66 \left(\frac{t_0}{l_0} \right)^3. \quad (6.15)$$

This implies that the singularity is globally naked for sufficiently small r_{sf} when t_0 and l_0 are fixed. Thus, it turns out that the present assumption $r_{sf}/l_0 \ll 1$ is relevant for the globally naked singularity case. We can translate the above condition to a condition for M and ω_s as

$$M \lesssim 6.4 \times 10^{-2} \omega_s^{-1}. \quad (6.16)$$

It implies that the mass of the dust cloud with the globally naked singularity is bounded from above.

D. Redshifts

Since it is necessary for later discussions, we turn our attention to redshifts of particles. Let k^μ be the tangent vector of a radial null geodesic. Inside of the dust cloud, k^μ satisfies the following equations:

$$-(k^t)^2 + (R_{,r})^2 (k^r)^2 = 0, \quad (6.17)$$

$$\frac{dk^t}{d\lambda} + R_{,r} R_{,tr} (k^r)^2 = 0, \quad (6.18)$$

$$\frac{d}{d\lambda} [(R_{,r})^2 k^r] - R_{,r} R_{,rr} (k^r)^2 = 0, \quad (6.19)$$

where λ is the affine parameter. The frequency $\hat{\omega}$ observed by an observer comoving with a fluid element is calculated from k^μ as

$$\hat{\omega} = -k^\mu u_\mu = -k^t. \quad (6.20)$$

In region A , Eqs. (6.17)-(6.19) can be integrated as

$$k^t (-\eta)^{2/3} \approx \text{const}, \quad (6.21)$$

$$k^r (-\eta)^{4/3} \approx \text{const} \quad (6.22)$$

in the lowest order. Therefore, a particle is blueshifted for the comoving observer in region A . In region B , Eqs. (6.17)-(6.19) can be integrated as

$$k^t \approx \text{const}, \quad (6.23)$$

$$k^r r^{4/3} \approx \text{const} \quad (6.24)$$

in the lowest order. Therefore a particle is neither redshifted nor blueshifted in region B .

In the external Schwarzschild spacetime, in a similar way, we obtain the tangent vector of a radial null geodesic as

$$k^T \left(1 - \frac{2M}{R} \right) = \text{const}, \quad (6.25)$$

$$k^R = \text{const}. \quad (6.26)$$

A static distant observer observes the frequency

$$\omega = -k^T(T, \infty). \quad (6.27)$$

Using the matching conditions (3.12)-(3.14), the observed frequency $\hat{\omega} = -k^\mu u_\mu$ by the comoving observer at the surface is written using the above ω as

$$\hat{\omega} = \frac{\omega}{1 \mp \alpha}, \quad (6.28)$$

where α is defined by

$$\alpha \equiv \sqrt{\frac{2M}{R}}, \quad (6.29)$$

and R is the areal radius of the dust surface when the null ray crosses the surface.

E. Estimate of function G or F

Let $\alpha_{0\pm}$ be the value of α for $n_{0\pm}$. Let $\eta_{0\pm}$ be the value of η when $n_{0\pm}$ crosses the dust surface. Then, from Eq. (3.16), it is easy to see that the Taylor expansion is valid around $\eta = \eta_{0-}$ for v as a function of η as

$$v = v_0 + \frac{1}{1 + \alpha_{0-}} (\eta - \eta_{0-}) + O((\eta - \eta_{0-})^2). \quad (6.30)$$

For $\alpha_{0+} < 1$, from Eq. (3.15), it is also easy to see that the Taylor expansion is valid around $\eta = \eta_{0+}$ for u as a function of η as

$$u = u_0 + \frac{1}{1 - \alpha_{0+}} (\eta - \eta_{0+}) + O((\eta - \eta_{0+})^2), \quad (6.31)$$

or equivalently,

$$\eta_{0+} - \eta = (1 - \alpha_{0+})(u_0 - u) + O((u_0 - u)^2). \quad (6.32)$$

See Fig. 9 again. An ingoing light ray which is close to $n_{0\pm}$ enters the dust cloud in region B (a), enters region A (b), crosses the center (c), becomes an outgoing light ray, enters again region B (d) and leaves the dust cloud (e). In

order to determine G or F , we need to relate the time coordinate η_a at which the incoming light ray enters the dust cloud with η_e at which the outgoing light ray leaves the dust cloud. Within the present approximation, the following relations hold:

$$\frac{\eta_{0-} - \eta_a}{t_0} \approx \frac{-\eta_b}{t_0} - 2^{-2/3} \gamma^{-7/6} \left(\frac{l_0}{t_0} \right) \left(\frac{-\eta_b}{t_0} \right)^{7/6}, \quad (6.33)$$

$$\left(\frac{-\eta_c}{t_0} \right)^{1/3} \approx \left(\frac{-\eta_b}{t_0} \right)^{1/3} - \frac{1}{3} \gamma^{-1/2} \left(\frac{l_0}{t_0} \right) \left(\frac{-\eta_b}{t_0} \right)^{1/2}, \quad (6.34)$$

$$\left(\frac{-\eta_c}{t_0} \right)^{1/3} \approx \left(\frac{-\eta_d}{t_0} \right)^{1/3} + \frac{1}{3} \gamma^{-1/2} \left(\frac{l_0}{t_0} \right) \left(\frac{-\eta_d}{t_0} \right)^{1/2}, \quad (6.35)$$

$$\frac{\eta_{0+} - \eta_e}{t_0} \approx \frac{-\eta_d}{t_0} + 2^{-2/3} \gamma^{-7/6} \left(\frac{l_0}{t_0} \right) \left(\frac{-\eta_d}{t_0} \right)^{7/6}, \quad (6.36)$$

where $\eta_{0\pm}$ are written as

$$\eta_{0\pm} \approx \pm 2^{-2/3} \left(\frac{l_0}{t_0} \right) \left(\frac{r_{sf}}{l_0} \right)^{7/3}. \quad (6.37)$$

From the above relations, we find

$$\eta_{0+} - \eta_e \approx \eta_{0-} - \eta_a. \quad (6.38)$$

Then, we find for $\alpha_{0+} < 1$

$$v = G(u) \approx v_0 - \frac{1 - \alpha_{0+}}{1 + \alpha_{0-}} (u_0 - u), \quad (6.39)$$

or

$$u = F(v) \approx u_0 - \frac{1 + \alpha_{0-}}{1 - \alpha_{0+}} (v_0 - v). \quad (6.40)$$

From the above discussions, we can determine $A = \lim_{u \rightarrow u_0} G'$ as

$$A = \frac{1 - \alpha_{0+}}{1 + \alpha_{0-}}. \quad (6.41)$$

For the collapse to a black hole, from Eq. (3.15), we can express u by η around $R = 2m$ at the surface as

$$u \approx -4M \ln(\eta_h - \eta) + \text{const}, \quad (6.42)$$

where η_h is the time when the event horizon crosses the dust surface. On the other hand, we can easily find the following linear relation when an incoming light ray with the advanced time v becomes to an outgoing null ray which reaches the surface at the time η as

$$\eta_h - \eta \approx \text{const} \times (v_h - v), \quad (6.43)$$

where the ingoing null ray with v_h is reflected to the outgoing ray on the event horizon. Then we find Eq. (4.27).

VII. VALIDITY OF THE GEOMETRICAL OPTICS APPROXIMATION

The geometrical optics approximation is exact for the two-dimensional spacetime, where the line element is given by setting $d\Omega^2 = 0$ in the four-dimensional line element (3.1). Therefore, the power, energy, and spectrum obtained in Secs. IV and V are exact in this sense for the two-dimensional version of the LTB spacetime.

In the four-dimensional case, the geometrical optics approximation is only an approximation because of the existence of the curvature potential. The geometrical optics approximation is valid for waves with the wavelength shorter than the curvature radius of the spacetime geometry. In other words, the geometrical optics approximation is good if condition

$$\hat{\omega} \gtrsim 2\pi |R_{\hat{\alpha}\hat{\beta}\hat{\gamma}\hat{\delta}}|^{1/2} \quad (7.1)$$

is satisfied, where the hat denotes components in the local inertial tetrad frame. The nonvanishing components of the Riemann tensor are as follows:

$$R_{\hat{t}\hat{r}\hat{t}\hat{r}} = -R_{\hat{t}\hat{r}\hat{r}\hat{t}} = -R_{\hat{r}\hat{t}\hat{t}\hat{r}} = R_{\hat{r}\hat{t}\hat{r}\hat{t}} = -\frac{R_{,ttr}}{R_{,r}}, \quad (7.2)$$

$$R_{\hat{t}\hat{\theta}\hat{t}\hat{\theta}} = -R_{\hat{t}\hat{\theta}\hat{\theta}\hat{t}} = -R_{\hat{\theta}\hat{t}\hat{t}\hat{\theta}} = R_{\hat{\theta}\hat{t}\hat{\theta}\hat{t}} = R_{\hat{t}\hat{\phi}\hat{t}\hat{\phi}} = -R_{\hat{t}\hat{\phi}\hat{\phi}\hat{t}} = -R_{\hat{\phi}\hat{t}\hat{t}\hat{\phi}} = R_{\hat{\phi}\hat{t}\hat{\phi}\hat{t}} = -\frac{R_{,tt}}{R}, \quad (7.3)$$

$$R_{\hat{r}\hat{\theta}\hat{r}\hat{\theta}} = -R_{\hat{r}\hat{\theta}\hat{\theta}\hat{r}} = -R_{\hat{\theta}\hat{r}\hat{r}\hat{\theta}} = R_{\hat{\theta}\hat{r}\hat{\theta}\hat{r}} = R_{\hat{r}\hat{\phi}\hat{r}\hat{\phi}} = -R_{\hat{r}\hat{\phi}\hat{\phi}\hat{r}} = -R_{\hat{\phi}\hat{r}\hat{r}\hat{\phi}} = R_{\hat{\phi}\hat{r}\hat{\phi}\hat{r}} = \frac{R_{,t}R_{,tr}}{RR_{,r}}, \quad (7.4)$$

$$R_{\hat{\theta}\hat{\phi}\hat{\theta}\hat{\phi}} = -R_{\hat{\theta}\hat{\phi}\hat{\phi}\hat{\theta}} = -R_{\hat{\phi}\hat{\theta}\hat{\theta}\hat{\phi}} = R_{\hat{\phi}\hat{\theta}\hat{\phi}\hat{\theta}} = \left(\frac{R_{,t}}{R}\right)^2. \quad (7.5)$$

In region A , they are approximated as

$$|R_{\hat{t}\hat{r}\hat{t}\hat{r}}| \approx |R_{\hat{t}\hat{\theta}\hat{t}\hat{\theta}}| \approx |R_{\hat{r}\hat{\theta}\hat{r}\hat{\theta}}| \approx |R_{\hat{\theta}\hat{\phi}\hat{\theta}\hat{\phi}}| \approx (-\eta)^{-2}. \quad (7.6)$$

In region B , they are approximated as

$$|R_{\hat{t}\hat{r}\hat{t}\hat{r}}| \approx |R_{\hat{t}\hat{\theta}\hat{t}\hat{\theta}}| \approx |R_{\hat{r}\hat{\theta}\hat{r}\hat{\theta}}| \approx |R_{\hat{\theta}\hat{\phi}\hat{\theta}\hat{\phi}}| \approx \frac{1}{t_0^2} \left(\frac{r}{l_0}\right)^{-4}. \quad (7.7)$$

In Sec. VID, we have seen that $\hat{\omega}$ is kept constant approximately in region B and that $\hat{\omega}$ may be considerably blueshifted in region A . However, in Sec. VIE, we can see that the null ray which goes into the dust cloud enters region A and get out of region A at the same time in the lowest order, i.e, $\eta_b \approx \eta_c \approx \eta_d$. This implies that the frequency of such a particle is kept almost constant all over the dust cloud. On the other hand, the Riemann tensor along the light ray reaches the maximum when the light ray goes through region A . Now we can write down the condition for the geometric optics approximation to be valid as

$$\hat{\omega} \gtrsim 2\pi(-\eta_c)^{-1}. \quad (7.8)$$

This condition can be rewritten by the quantities on \mathfrak{S}^+ using Eqs. (6.28) and (6.31). The result is

$$\omega \gtrsim \omega_{cr}(u) \equiv 2\pi(u_0 - u)^{-1} \quad (7.9)$$

for $\alpha_{0+} < 1$.

As we have shown in Sec. V, the power for each mode is mainly transported by particles of which the frequency is about $2\pi(u_0 - u)^{-1}$. Since the transmission coefficient Γ_ω will be a function of (ω/ω_{cr}) , it is natural to estimate $\Gamma_\omega(\omega = \omega_{cr})$ as of the order unity. It implies that the calculations based on the geometrical optics approximation will be valid for a rough order estimate.

VIII. DISCUSSIONS

Here we compare the naked singularity explosion with the famous radiative phenomena, the Hawking radiation, and the black hole evaporation. The Hawking radiation is derived in the fixed background spacetime as has been done in this paper. The result is thermal radiation, the temperature of which is given by

$$T = \frac{1}{8\pi M}, \quad (8.1)$$

and the power is given by

$$P = \hat{P} = \frac{1}{768\pi M^2}. \quad (8.2)$$

The Hawking radiation is not explosive but constant.

In contrast to the naked singularity explosion, it is not until the back reaction of the quantum effect is taken into account that explosive radiation is emitted. For the black hole evaporation, the power is given by

$$P \sim (t_{ev} - t)^{-2/3}, \quad (8.3)$$

where t_{ev} is the time of evaporation and the above equation is valid only for $t_{ev} - t > 1$, where 1 means, of course, the Planck time. The divergence is apparently much milder than the naked singularity explosion. The expression of the power does not have any parameter dependence. The radiated energy during the final evaporation phase is only finite in contrast to the naked singularity. The mass of the evaporating black hole is given by

$$M \sim (t_{ev} - t)^{1/3}. \quad (8.4)$$

From the above equations, the power at the time t is dominated by particles with frequency

$$\omega \sim (t_{ev} - t)^{-1/3}. \quad (8.5)$$

The total spectrum is estimated from Eqs. (8.3) and (8.5) as

$$\omega \frac{dN}{d\omega} \sim \omega^{-2}, \quad (8.6)$$

where this estimate is valid for $\omega < 1$. Equation (8.6) implies that the spectrum is apparently softer than that of the naked singularity explosion. For the Hawking radiation, since the Schwarzschild black hole has only one parameter, i.e., its mass, the back reaction effect is rather easy to be taken into account although it is phenomenological. For the naked singularity, the system is dynamical and not parametrized by only one parameter. It suggests that it is not an easy task to take the back reaction of the quantum effect into account even phenomenologically. The comparison of radiation processes in the collapse of a dust ball is shown in Table I.

TABLE I. Comparison of radiation processes: Hawking radiation (HR), black hole evaporation (BHE), naked singularity explosion (NSE) [24], and naked singularity explosion in self-similar spacetime (NSESS) [18–20].

Process	HR	BHE	NSE	NSESS
Radiation	Constant	Explosive	Explosive	Explosive
P (total div. subtracted)	$(768\pi M^2)^{-1}$	$\sim (t_{ev} - t)^{-2/3}$	$\sim \nu_s (t_{CH} - t)^{-1}$	$\sim (t_{CH} - t)^{-2}$
E	$\sim (768\pi M^2)^{-1} t$	M	$\sim \nu_s \log(t_{CH} - t)$	$\sim (t_{CH} - t)^{-1}$
$\nu \frac{dN}{d\nu}$	$\frac{\nu}{e^{16\pi^2 M \nu} - 1}$	$\sim \nu^{-2}$	$\sim \left(\frac{\nu}{\nu_s}\right)^{-1}$?
$\langle \nu \rangle$	$\sim M^{-1}$	$\sim (t_{ev} - t)^{-1/3}$	$\sim (t_{CH} - t)^{-1}$?
Back reaction		$\frac{dM}{dt} = -P$		
Geometrical approx.	Good	Good	Marginal	?
Redshift	∞	∞	Finite	∞

Again we return to the naked singularity explosion. The singularity frequency ω_s is obtained from Eq. (4.9) as

$$\omega_s \sim 10^{-3} \left(\frac{t_0}{1\text{ms}} \right)^{-7} \left(\frac{l_0}{10\text{km}} \right)^6 \text{ Hz.} \quad (8.7)$$

The characteristic frequency depends not only on the free fall time of the system but also greatly on the scale of inhomogeneity. The scale of inhomogeneity becomes larger, the singularity frequency becomes higher. In some situations, gravitational collapse will set in due to the growth of small perturbations of hydrostatic equilibrium in a Newtonian regime. In such a case, t_0 and l_0 will be related as $l_0/t_0 = \sqrt{15}c_s$, where c_s is the sound speed at the center. Then the singularity frequency is given by $\omega_s \sim 10^3 c_s^6 t_0^{-1}$. It implies that ω_s does not much exceed the inverse of the initial free fall time in such situations.

From Eq. (5.16), it is found that

$$N \sim \int_{\omega_{tp}}^{\infty} d\omega \frac{dN}{d\omega} \sim \frac{\omega_s}{\omega_{tp}} \sim (M\omega_s)^{2/3} \lesssim 1. \quad (8.8)$$

Thus, the total number of emitted particles with frequency above ω_{tp} is a few at most. It suggests that the radiation may be extremely directional because a few particles transport almost all the energy radiated during the collapse.

We are not sure how to take into account the back reaction of the quantum effect. However, we can assume that the back reaction of the quantum effect becomes important if a considerable fraction of the total energy of the system are radiated away by the quantum particle creation. From this assumption, we can estimate the emitted energy as $E \sim 10^{54}(M/M_\odot)\text{erg}$, although M must satisfy condition (6.16). For $E = fM$ with $f \lesssim 1$, the averaged energy ω_{av} of the radiated particles above ω_{tp} is given by

$$\omega_{av} \sim E/N \sim E(M\omega_s)^{-2/3} \sim fM^{1/3}\omega_s^{-2/3}. \quad (8.9)$$

The central energy density ϵ_c at the final stage is given by

$$\epsilon_c \sim \omega_{tp}^2 \exp\left(\frac{2E}{\omega_s}\right) \sim M^{-4/3}\omega_s^{2/3} \exp\left(\frac{2E}{\omega_s}\right), \quad (8.10)$$

because Δt is given by

$$\Delta t \sim \omega_{tp}^{-1} \exp\left(-\frac{E}{\omega_s}\right) \sim M^{2/3}\omega_s^{-1/2} \exp\left(-\frac{E}{\omega_s}\right). \quad (8.11)$$

Actually, this estimate for the radiated energy should be considered as an upper bound. It is noted that we have to transform these intrinsic quantities to observed quantities by considering possible reactions of created energetic particles.

The naked singularity explosion may be a new candidate for a source of ultrahigh energy cosmic rays because it has a potentially extremely hard spectrum. It may also provide a candidate for a central engine of γ -ray bursts. The naked singularity explosion could contribute γ -ray background radiation or disturb big bang nucleosynthesis.

IX. CONCLUSIONS

We have considered the naked singularity which occurs in the collapse of a dust ball with the initial density profile which is physically reasonable. We have calculated radiation during the naked singularity formation under the geometrical optics approximation. Since the regularization in these calculations has been done only in a flat spacetime, the results contain no ambiguity which could come from local curvature. We have obtained the power and energy of the radiation, which turn out to diverge to positive infinity for both minimally and conformally coupled massless scalar fields. We have also obtained the spectrum of radiation, both total and momentary ones. Then we have found that the power is dominantly contributed from particles of frequency $\omega \sim 2\pi(t_{\text{CH}} - t)^{-1}$, where $(t_{\text{CH}} - t)$ is the remaining time until a distant observer could see the singularity. The spectrum is given by $\omega dN/d\omega \approx (\omega/\omega_s)^{-1}$, which is much harder than that of the black hole evaporation. The radiation depends on the characteristic frequency ω_s of the singularity, which is determined by the initial free fall time and the initial scale of inhomogeneity at the center. The radiation may be expected to be strongly beamed. The geometrical optics approximation has turned out to be consistent for a rough order estimate. It will provide a very interesting candidate for a central engine of γ -ray bursts or a source of ultrahigh energy cosmic rays because the predicted intrinsic spectrum may be extended to an extremely high frequency. A detailed study on such astrophysical implications will be a future work.

After this manuscript was received, the paper [34] appeared, in which the naked singularity formation is discussed as a possible origin of γ -ray bursts.

ACKNOWLEDGMENTS

We are grateful to H. Sato for his continuous encouragement. We are also grateful to T. Nakamura, H. Kodama, T.P. Singh, A. Ishibashi, and S.S. Deshingkar for helpful discussions. This work was supported by the Grant-in-Aid for Scientific Research (No. 05540) and for Creative Basic Research (No. 09NP0801) from the Japanese Ministry of Education, Science, Sports, and Culture.

APPENDIX A: CONSERVED QUANTITY IN LTB COLLAPSE

In Sec. III, we set the initial data at $t = 0$ and specified the solution. In fact, the choice of an initial slice is arbitrary. Therefore, another slice among the synchronous comoving slicings can be chosen as an initial slice. Since this variety of choices of an initial slice, of course, does not change the original collapse model, physical quantities, such as, power and energy, must not depend on the choice of an initial slice.

At an arbitrary time $t < t_0$, using Eqs. (3.8) and (6.1), we can expand the mass function $F(r)$ in terms of the areal radius R as

$$F(r) = F_3 \left(\frac{-\eta}{t_0} \right)^{-2} R^3 + F_5 \left(\frac{-\eta}{t_0} \right)^{-13/3} R^5 + \dots \quad (\text{A1})$$

We can define the coefficients of R^3 and R^5 as $\tilde{F}_3(\eta)$ and $\tilde{F}_5(\eta)$. Then we can define the free fall time $\tilde{t}_0(\eta)$ and the scale of inhomogeneity $\tilde{l}_0(\eta)$ at the time η as

$$\tilde{t}_0(\eta) \equiv \frac{2}{3} (\tilde{F}_3(\eta))^{-1/2} = t_0 \left(\frac{-\eta}{t_0} \right), \quad (\text{A2})$$

$$\tilde{l}_0(\eta) \equiv \left(\frac{-\tilde{F}_5(\eta)}{\tilde{F}_3(\eta)} \right)^{-1/2} = l_0 \left(\frac{-\eta}{t_0} \right)^{7/6}, \quad (\text{A3})$$

where t_0 and l_0 are understood as $\tilde{t}_0(0)$ and $\tilde{l}_0(0)$, respectively. Then we can easily find that the following quantity is independent of the choice of an initial slice.

$$\frac{\tilde{t}_0(\eta)^7}{\tilde{l}_0(\eta)^6} = \frac{t_0^7}{l_0^6} = \text{const.} \quad (\text{A4})$$

APPENDIX B: ANALYTIC EXPRESSIONS OF BOGOLIUBOV COEFFICIENTS

As seen in Sec. VI, for $\alpha_{0+} < 1$, we can write the function $F(v)$ in the following form

$$F(v) \approx u_0 - a(v_0 - v) + b(v_0 - v)^\delta, \quad (\text{B1})$$

where δ , a and b satisfy

$$\delta = \frac{3}{2}, \quad (\text{B2})$$

$$a > 0, \quad (\text{B3})$$

$$b > 0. \quad (\text{B4})$$

We denote the advanced time as $v = v_0 - d$ after which the higher-order terms can be neglected, where $d = O(b^{-1/(\delta-1)})$ is satisfied. Because the particle creation will occur due to the third term in the right-hand side of Eq. (B1), the dominant contribution to the spectrum comes from the integral on $v_0 - d < v < v_0$ in Eqs. (2.15) and (2.16). Then, the Bogoliubov coefficients are obtained from Eqs. (2.15) and (2.16) as

$$\alpha_{\omega'\omega} \approx \frac{1}{2\pi} \sqrt{\frac{\omega'}{\omega}} e^{i\omega u_0 - i\omega' v_0} \int_0^d e^{-i\omega(as - bs^\delta) + i\omega's} ds, \quad (\text{B5})$$

$$\beta_{\omega'\omega} \approx -\frac{1}{2\pi} \sqrt{\frac{\omega'}{\omega}} e^{-i\omega u_0 - i\omega' v_0} \int_0^d e^{i\omega(as - bs^\delta) + i\omega's} ds. \quad (\text{B6})$$

They have the following expression

$$\alpha_{\omega'\omega} \approx \frac{1}{2\pi\sqrt{\omega\omega'}} e^{i\omega u_0 - i\omega' v_0} \sum_{k=0}^{\infty} \sum_{j=0}^k (-1)^j i^k \frac{C_j^k}{k!} a^j \frac{\omega^k c^{(\delta-1)(k-j)}}{(\omega')^{k+(\delta-1)(k-j)}} \int_0^{\omega'd} dx e^{ix} x^{j+\delta(k-j)}, \quad (\text{B7})$$

$$\beta_{\omega'\omega} \approx -\frac{1}{2\pi\sqrt{\omega\omega'}} e^{-i\omega u_0 - i\omega' v_0} \sum_{k=0}^{\infty} \sum_{j=0}^k (-1)^{k-j} i^k \frac{C_j^k}{k!} a^j \frac{\omega^k c^{(\delta-1)(k-j)}}{(\omega')^{k+(\delta-1)(k-j)}} \int_0^{\omega'd} dx e^{ix} x^{j+\delta(k-j)}, \quad (\text{B8})$$

where we have introduced the frequency c which characterizes the singularity as

$$c \equiv b^{1/(\delta-1)}. \quad (\text{B9})$$

They also have another expansion:

$$\alpha_{\omega'\omega} \approx \frac{1}{2\pi} \sqrt{\frac{\omega'}{\omega}} e^{i\omega u_0 - i\omega' v_0} \frac{1}{a\omega} \sum_{k=0}^{\infty} \sum_{j=0}^k i^k \frac{C_j^k}{k!} \frac{1}{a^{j+(\delta-1)(k-j)}} \frac{(\omega')^j c^{(\delta-1)(k-j)}}{\omega^{j+(\delta-1)(k-j)}} \int_0^{a\omega d} dx e^{-ix} x^{j+\delta(k-j)}, \quad (\text{B10})$$

$$\beta_{\omega'\omega} \approx -\frac{1}{2\pi} \sqrt{\frac{\omega'}{\omega}} e^{-i\omega u_0 - i\omega' v_0} \frac{1}{a\omega} \sum_{k=0}^{\infty} \sum_{j=0}^k (-1)^{(2\delta-1)(k-j)} i^k \frac{C_j^k}{k!} \frac{1}{a^{j+(\delta-1)(k-j)}} \frac{(\omega')^j c^{(\delta-1)(k-j)}}{\omega^{j+(\delta-1)(k-j)}} \int_0^{a\omega d} dx e^{ix} x^{j+\delta(k-j)}. \quad (\text{B11})$$

They also have another expansion:

$$\alpha_{\omega'\omega} \approx \frac{1}{2\pi} \sqrt{\frac{\omega'}{\omega}} e^{i\omega u_0 - i\omega' v_0} \frac{1}{\delta\omega} \sum_{k=0}^{\infty} \frac{i^k}{k!} \left(\frac{\omega'}{\omega} - a\right)^k \left(\frac{\omega}{c}\right)^{(1+k)(1-\frac{1}{\delta})} \int_0^{\frac{\omega}{c}(cd)^\delta} dx e^{ix} x^{\frac{1+k}{\delta}}, \quad (\text{B12})$$

$$\beta_{\omega'\omega} \approx \frac{1}{2\pi} \sqrt{\frac{\omega'}{\omega}} e^{-i\omega u_0 - i\omega' v_0} \frac{1}{\delta\omega} \sum_{k=0}^{\infty} \frac{i^k}{k!} \left(\frac{\omega'}{\omega} + a\right)^k \left(\frac{\omega}{c}\right)^{(1+k)(1-\frac{1}{\delta})} \int_0^{\frac{\omega}{c}(cd)^\delta} dx e^{-ix} x^{\frac{1+k}{\delta}}. \quad (\text{B13})$$

For $\omega' \rightarrow 0$, as seen in Eqs. (B7) and (B8), they behave as

$$\alpha_{\omega'\omega} \approx \frac{i}{2\pi\sqrt{\omega\omega'}} e^{i\omega u_0 - i\omega' v_0}, \quad (\text{B14})$$

$$\beta_{\omega'\omega} \approx -\frac{i}{2\pi\sqrt{\omega\omega'}} e^{-i\omega u_0 - i\omega' v_0}. \quad (\text{B15})$$

For $\omega' \rightarrow \infty$, as seen in Eqs. (B10) and (B11), they behave as

$$\alpha_{\omega'\omega} \approx \frac{1}{2\pi} \frac{(\omega')^{1/2}}{a\omega^{3/2}} e^{i\omega u_0} \int_0^{a\omega d} dx e^{-ix}, \quad (\text{B16})$$

$$\beta_{\omega'\omega} \approx \frac{1}{2\pi} \frac{(\omega')^{1/2}}{a\omega^{3/2}} e^{-i\omega u_0} \int_0^{a\omega d} dx e^{ix}, \quad (\text{B17})$$

where we have used the formula

$$\int_0^\infty dx e^{-(\epsilon+ia)x} x^{z-1} = \frac{\Gamma(z)}{(\epsilon+ia)^z}, \quad (\text{B18})$$

for $\epsilon > 0$ and $z > 0$.

- [1] D.M. Eardley and L. Smarr, Phys. Rev. D **19**, 2239 (1979).
- [2] D. Christodoulou, Commun. Math. Phys. **93**, 171 (1984).
- [3] R.P.A.C. Newman, Class. Quantum Grav. **3**, 527 (1986).
- [4] P.S. Joshi and I.H. Dwivedi, Phys. Rev. D **47**, 5357 (1993).
- [5] A. Ori and T. Piran, Phys. Rev. Lett. **59**, 2137 (1987).
- [6] A. Ori and T. Piran, Gen. Relativ. Gravit. **20**, 7 (1988).
- [7] A. Ori and T. Piran, Phys. Rev. D **42**, 1068 (1990).
- [8] T. Harada, Phys. Rev. D **58**, 104015 (1998).
- [9] S.L. Shapiro and S.A. Teukolsky, Phys. Rev. Lett. **66**, 994 (1991).
- [10] S.L. Shapiro and S.A. Teukolsky, Phys. Rev. D **45**, 2006 (1992).
- [11] T. Nakamura, M. Shibata, and K. Nakao, Prog. Theor. Phys. **89**, 821 (1993).
- [12] H. Iguchi, K. Nakao, and T. Harada, Phys. Rev. D **57**, 7262 (1998).
- [13] H. Iguchi, T. Harada, and K. Nakao, Prog. Theor. Phys. **101**, 1235 (1999).
- [14] H. Iguchi, T. Harada, and K. Nakao, Prog. Theor. Phys. **103**, 53 (2000).
- [15] S.W. Hawking, Commun. Math. Phys. **43**, 199 (1975).
- [16] L.H. Ford and L. Parker, Phys. Rev. D **17**, 1485, (1978)
- [17] W.A. Hiscock, L.G. Williams, and D.M. Eardley, Phys. Rev. D **26**, 751 (1982).
- [18] S. Barve, T.P. Singh, C. Vaz, and L. Witten, Nucl. Phys. **B532**, 361 (1998).
- [19] S. Barve, T.P. Singh, C. Vaz, and L. Witten, Phys. Rev. D **58**, 104018 (1998).
- [20] C. Vaz and L. Witten, Phys. Lett. B **442**, 90 (1998).
- [21] S.S. Deshingkar, P.S. Joshi, and I.H. Dwivedi, Phys. Rev. D **59**, 044018 (1999).
- [22] T. Harada, K. Nakao, and H. Iguchi, Class. Quantum Grav. **16**, 2785 (1999).
- [23] I.H. Dwivedi, Phys. Rev. D **58**, 064004 (1998).
- [24] T. Harada, H. Iguchi and K. Nakao, Phys. Rev. D **61**, 101502 (2000).
- [25] C.W. Misner, K.S. Thorne, and J.A. Wheeler, *Gravitation* (Freeman, San Francisco, 1973).
- [26] N.D. Birrel and P.C.W. Davies, *Quantum Fields in Curved Space* (Cambridge University Press, Cambridge, England, 1984).
- [27] R.C. Tolman, Proc. Natl. Acad. Sci. **20**, 169 (1934).
- [28] H. Bondi, Mon. Not. R. Astron. Soc. **107**, 410 (1947).
- [29] T.P. Singh and P.S. Joshi, Class. Quantum Grav. **13**, 559 (1996).
- [30] S. Jhingan, P.S. Joshi, and T.P. Singh, Class. Quantum Grav. **13**, 3057 (1996).
- [31] S. Jhingan and P.S. Joshi, Ann. Isr. Phys. Soc. **13**, 357 (1997).
- [32] F.J. Tipler, Phys. Lett. **64A**, 8 (1977).
- [33] A. Królak, J. Math. Phys. **28**, 138 (1987).
- [34] P.S. Joshi, N. Dadhich, and R. Maartens, Mod. Phys. Lett. A **15**, 991 (2000).

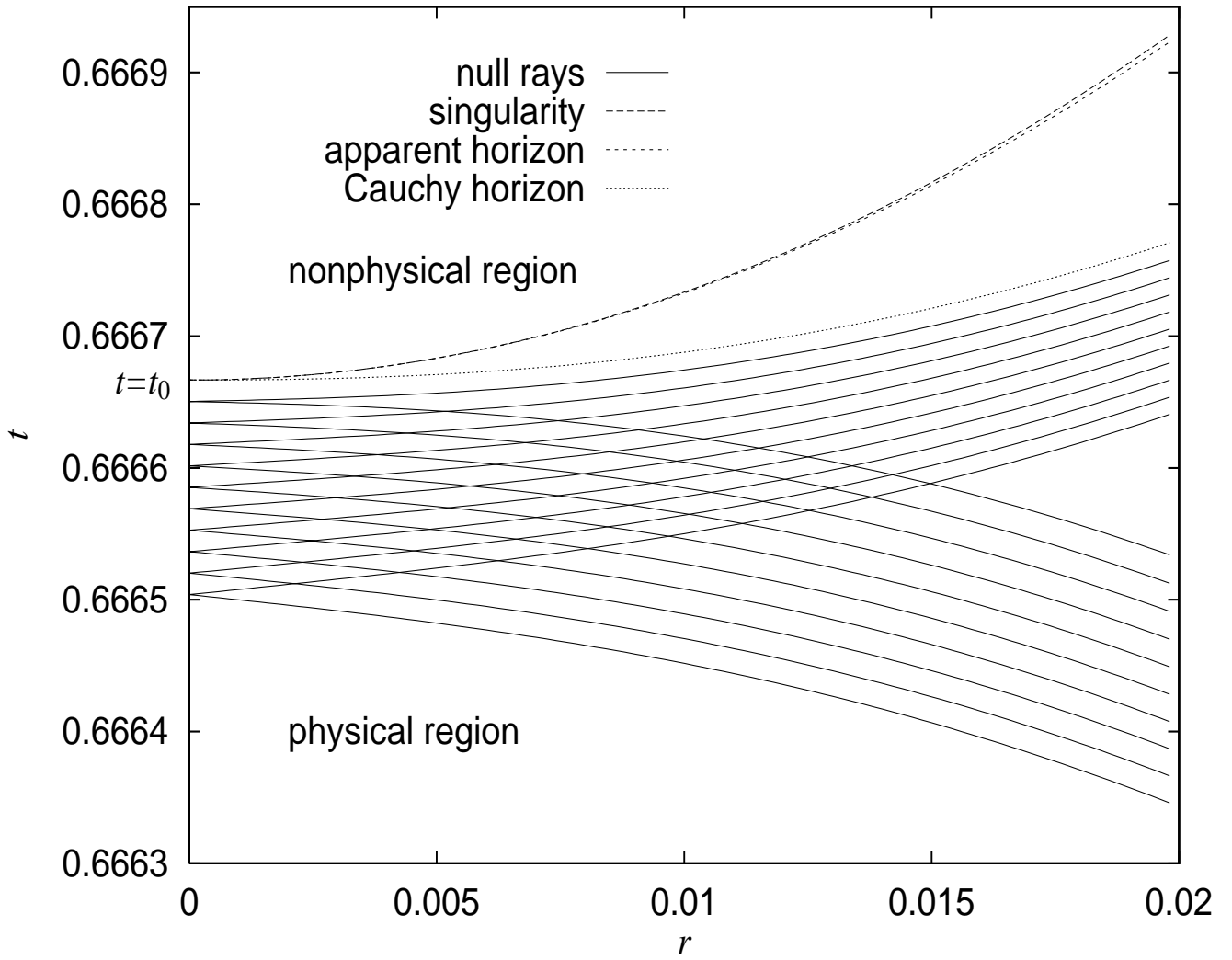
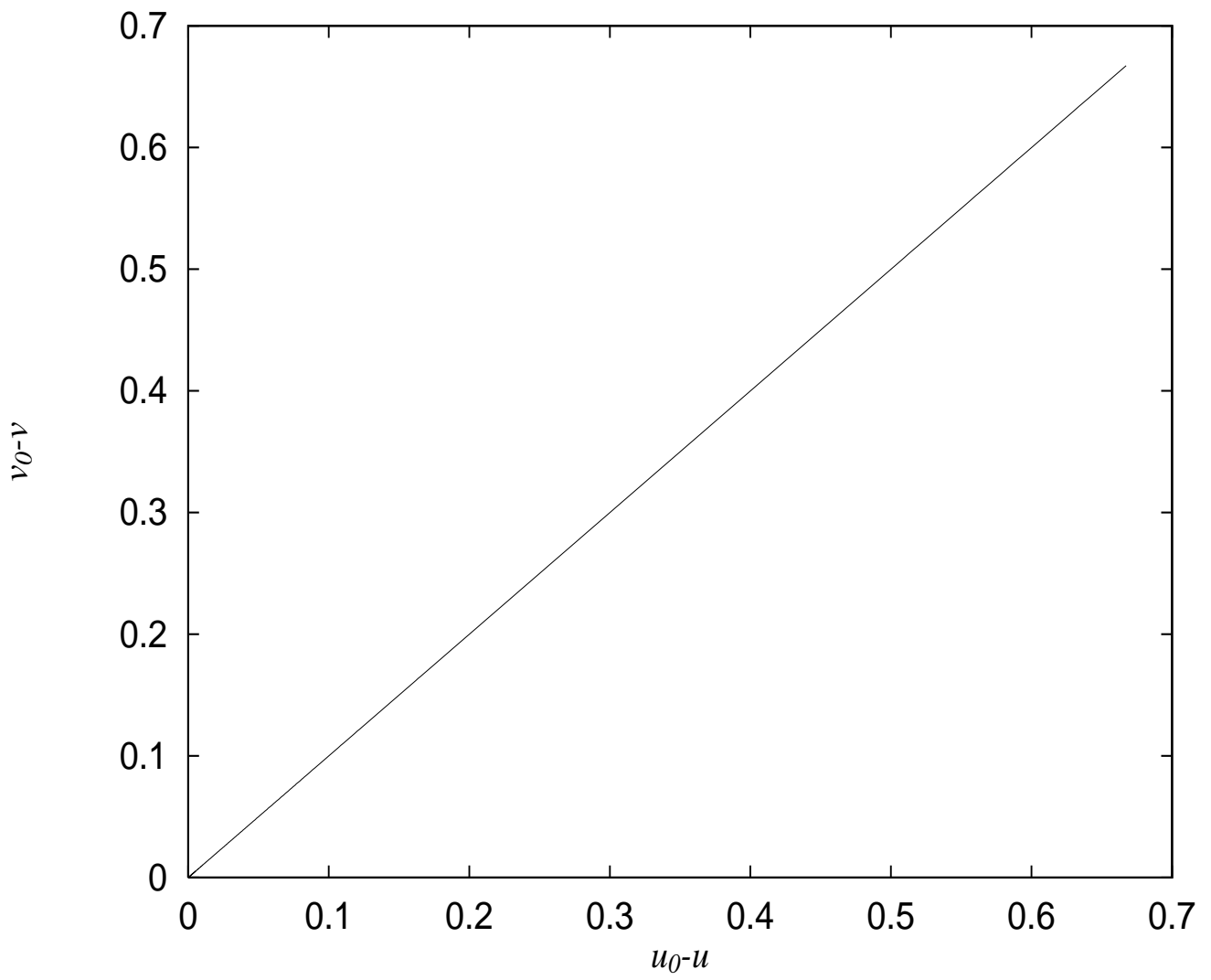
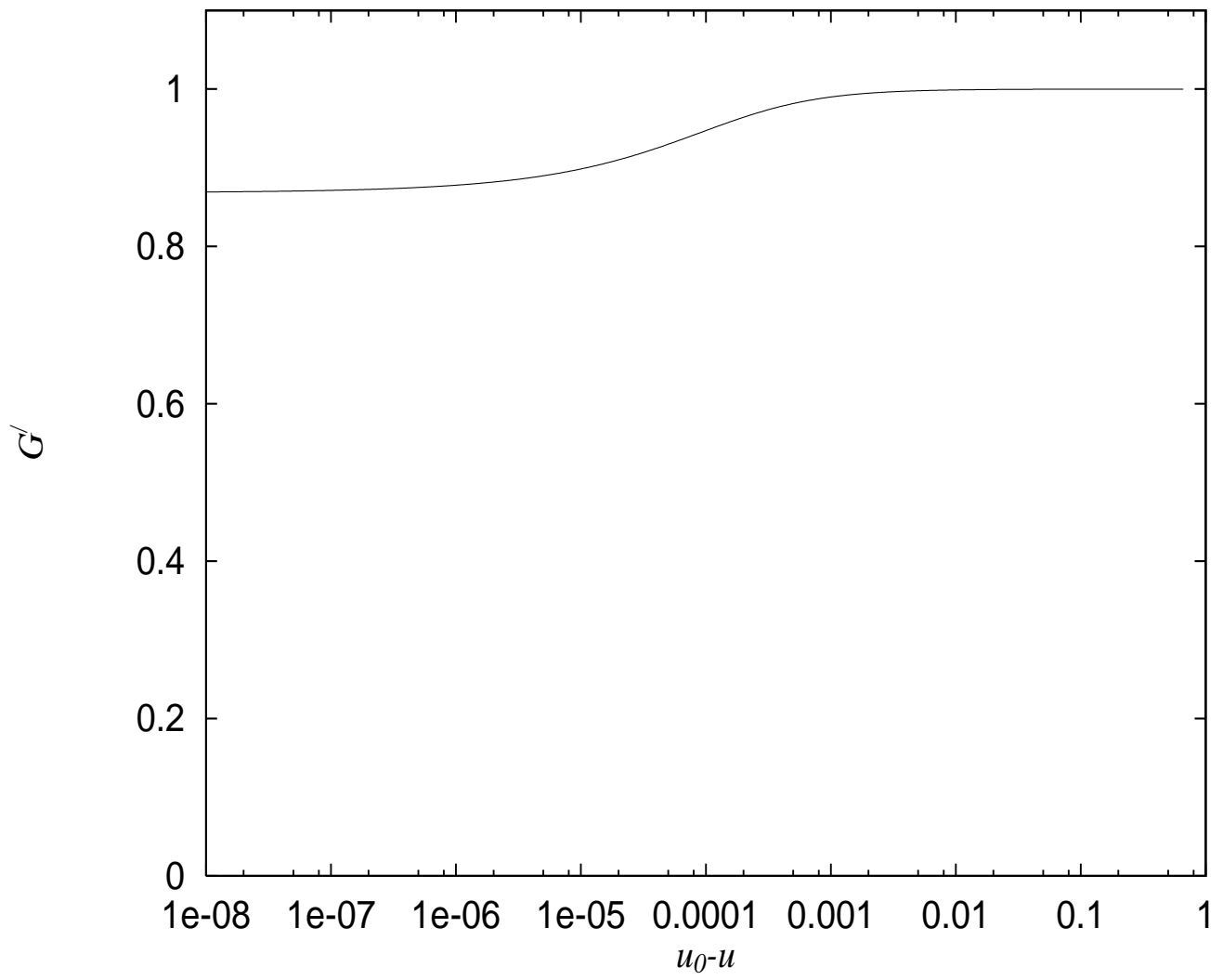


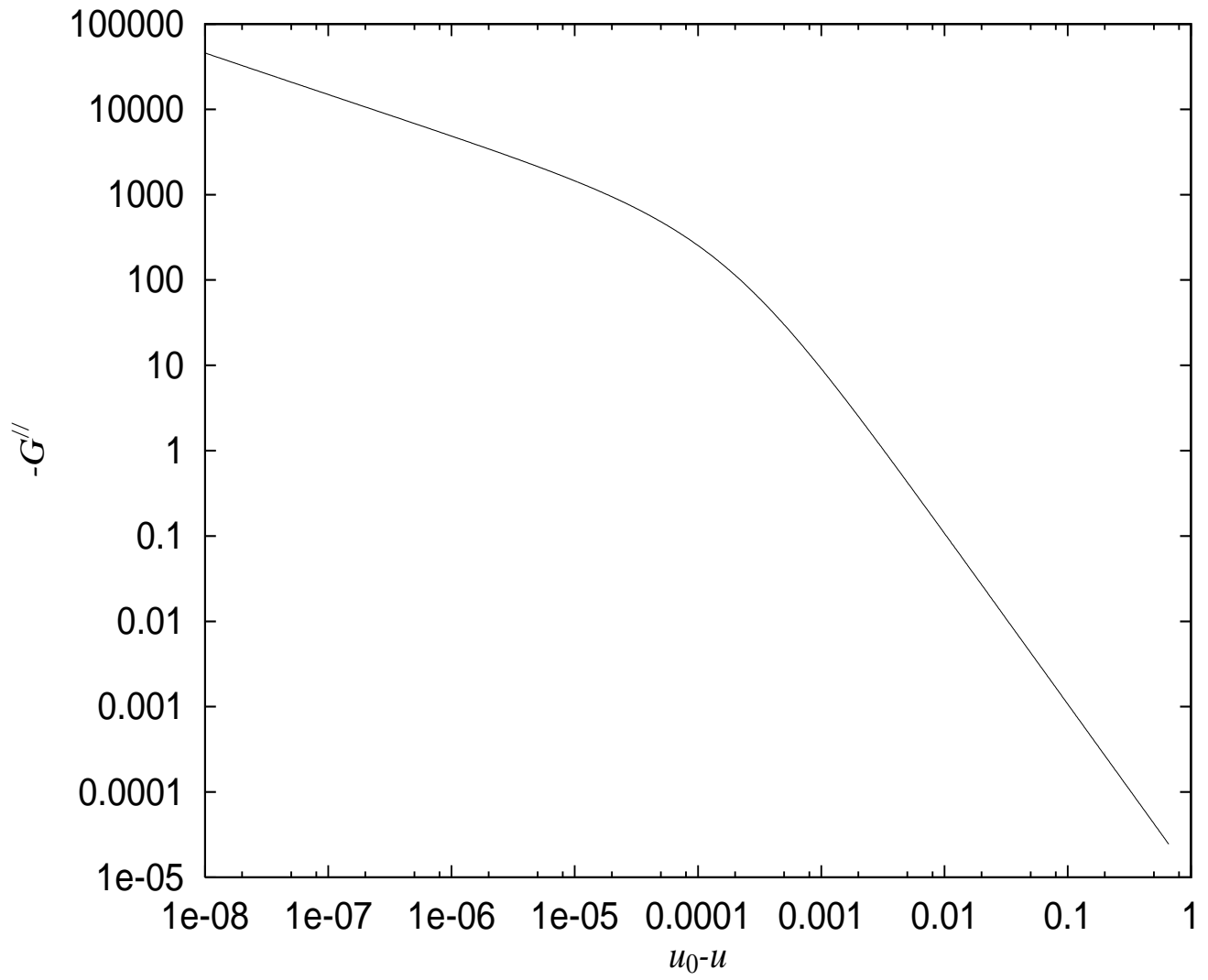
FIG. 1. Null rays interior of the dust cloud in the LTB spacetime.



(a)



(b)



(c)

FIG. 2. Plots of (a) $G(u)$, and (b) $G'(u)$, (c) $G''(u)$ for the LTB spacetime.

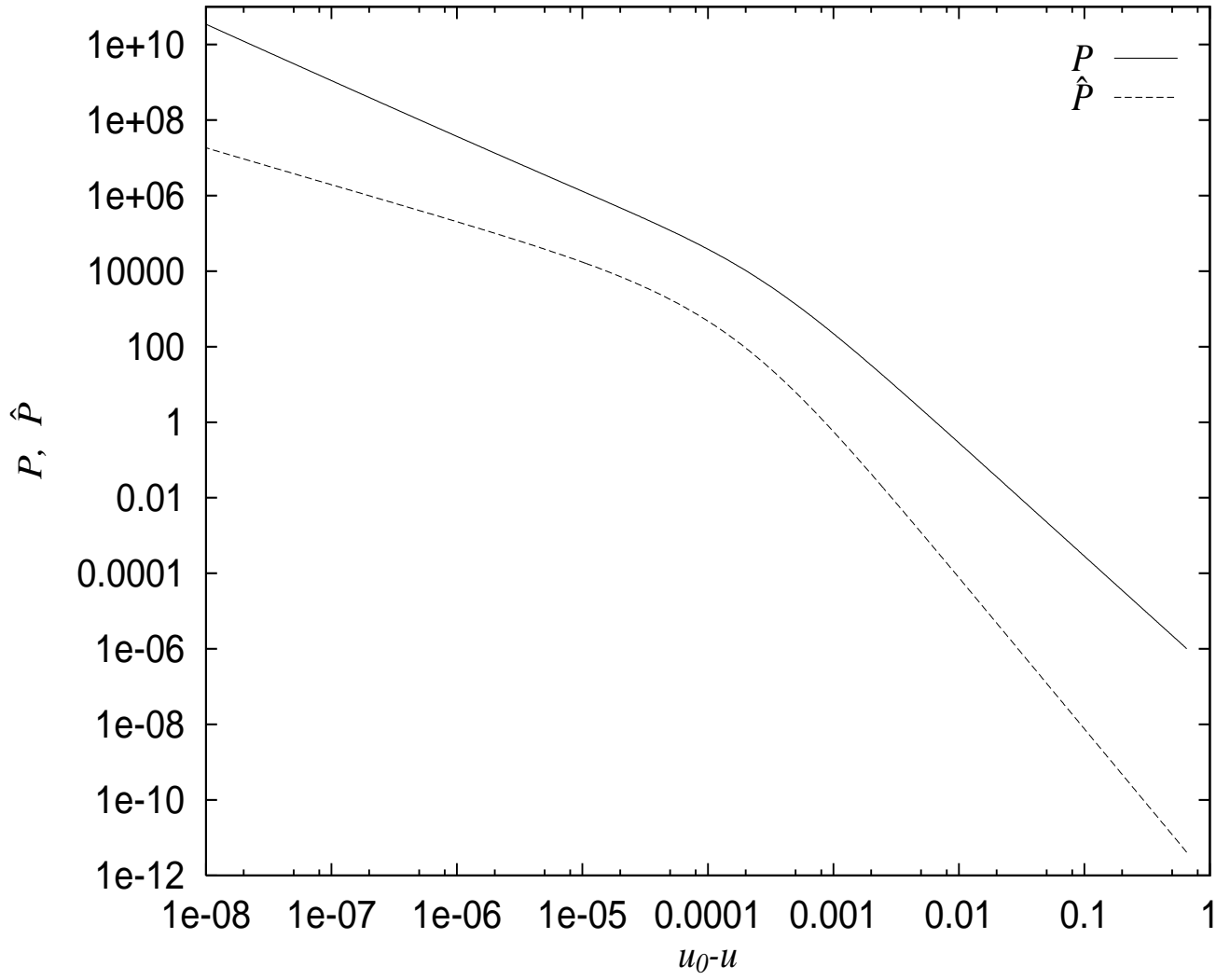


FIG. 3. Power for minimally and conformally coupled scalar fields in the LTB spacetime

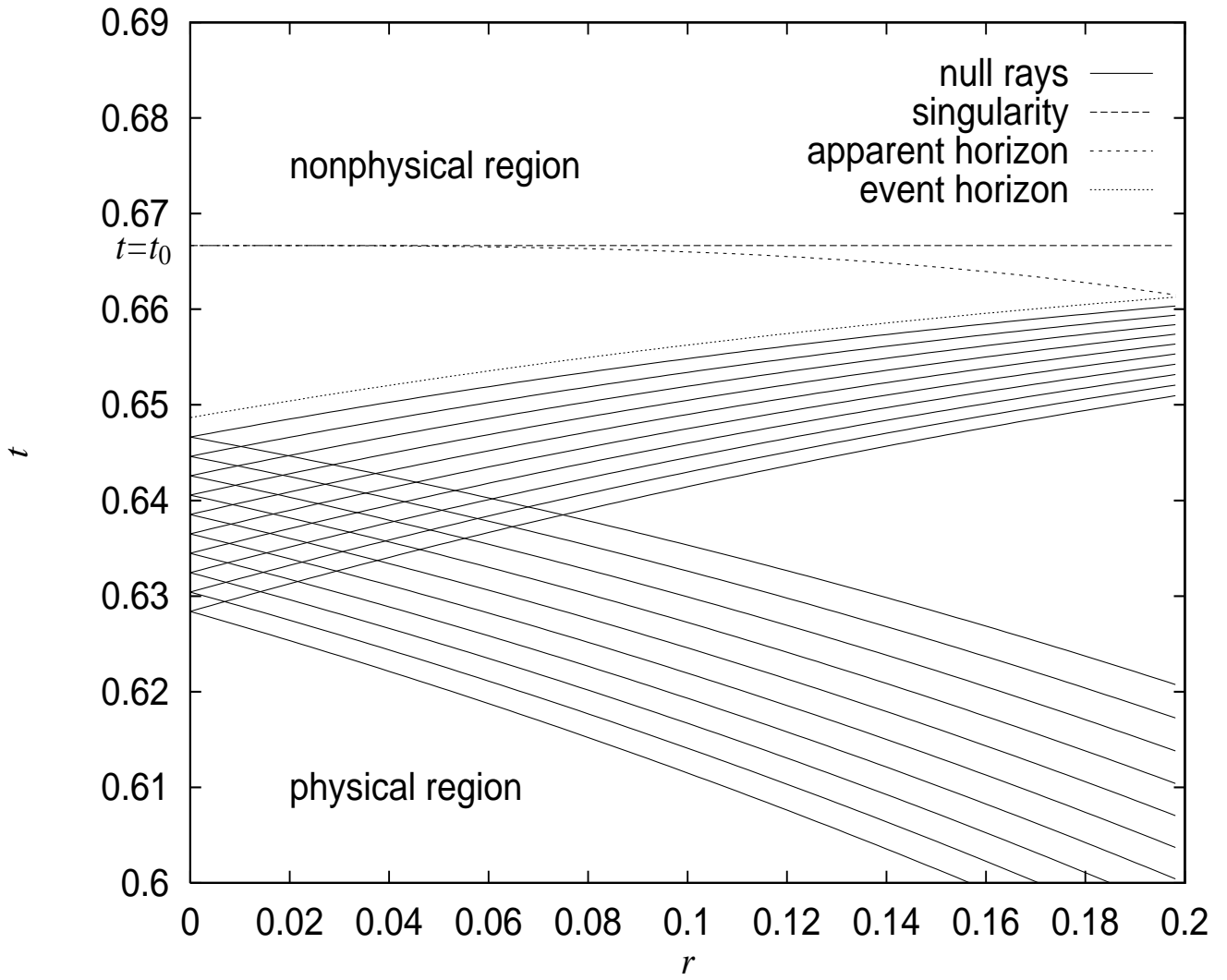
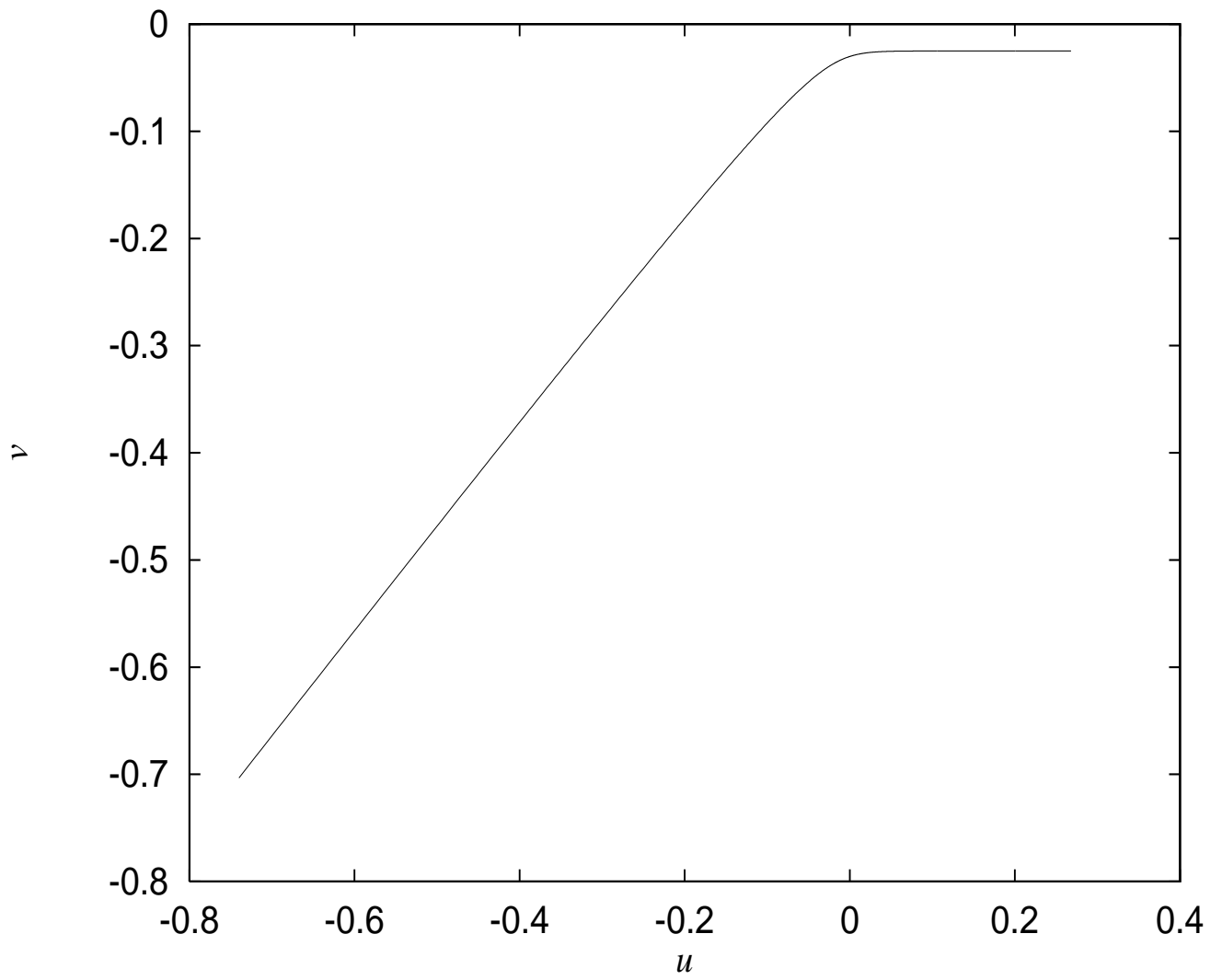
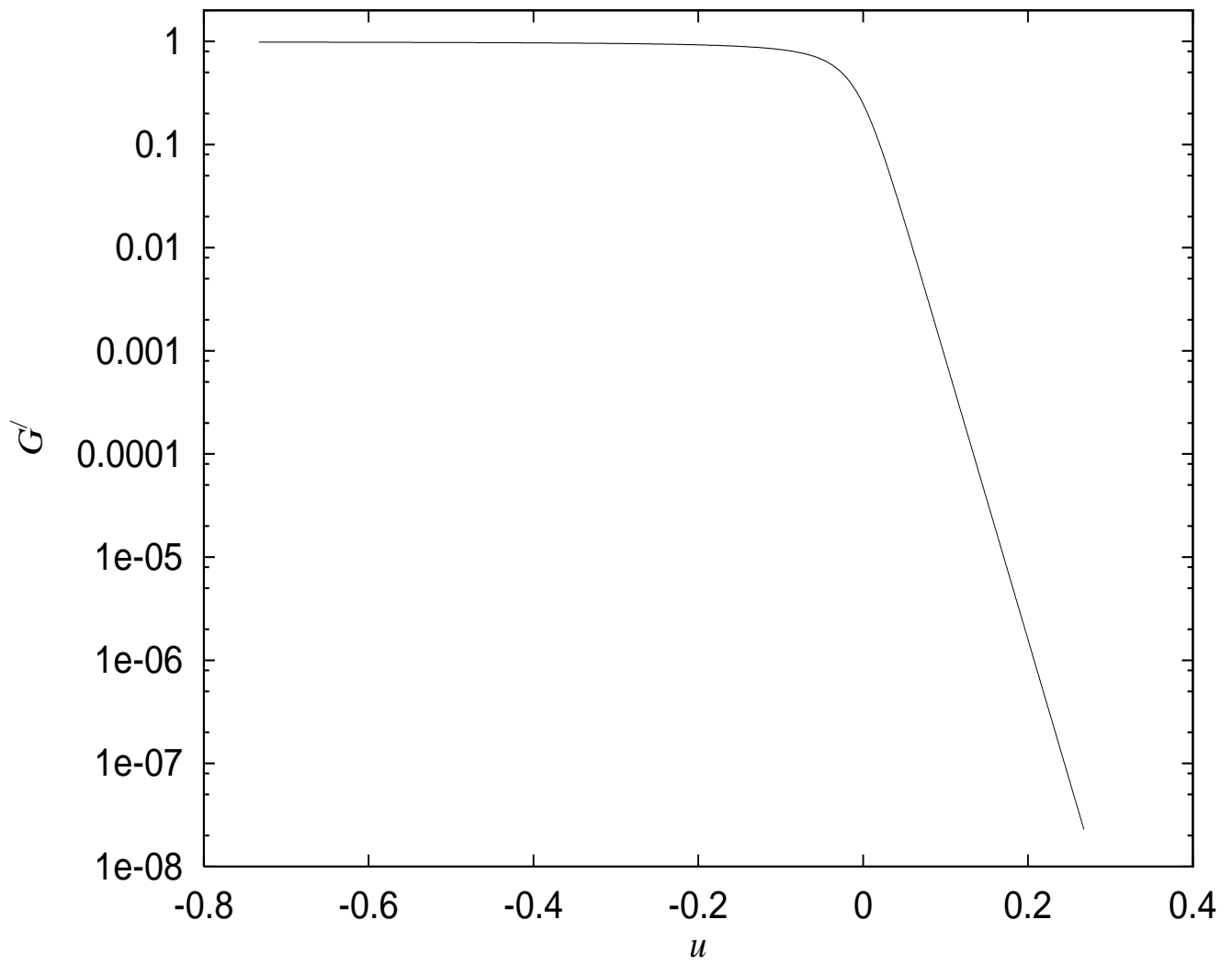


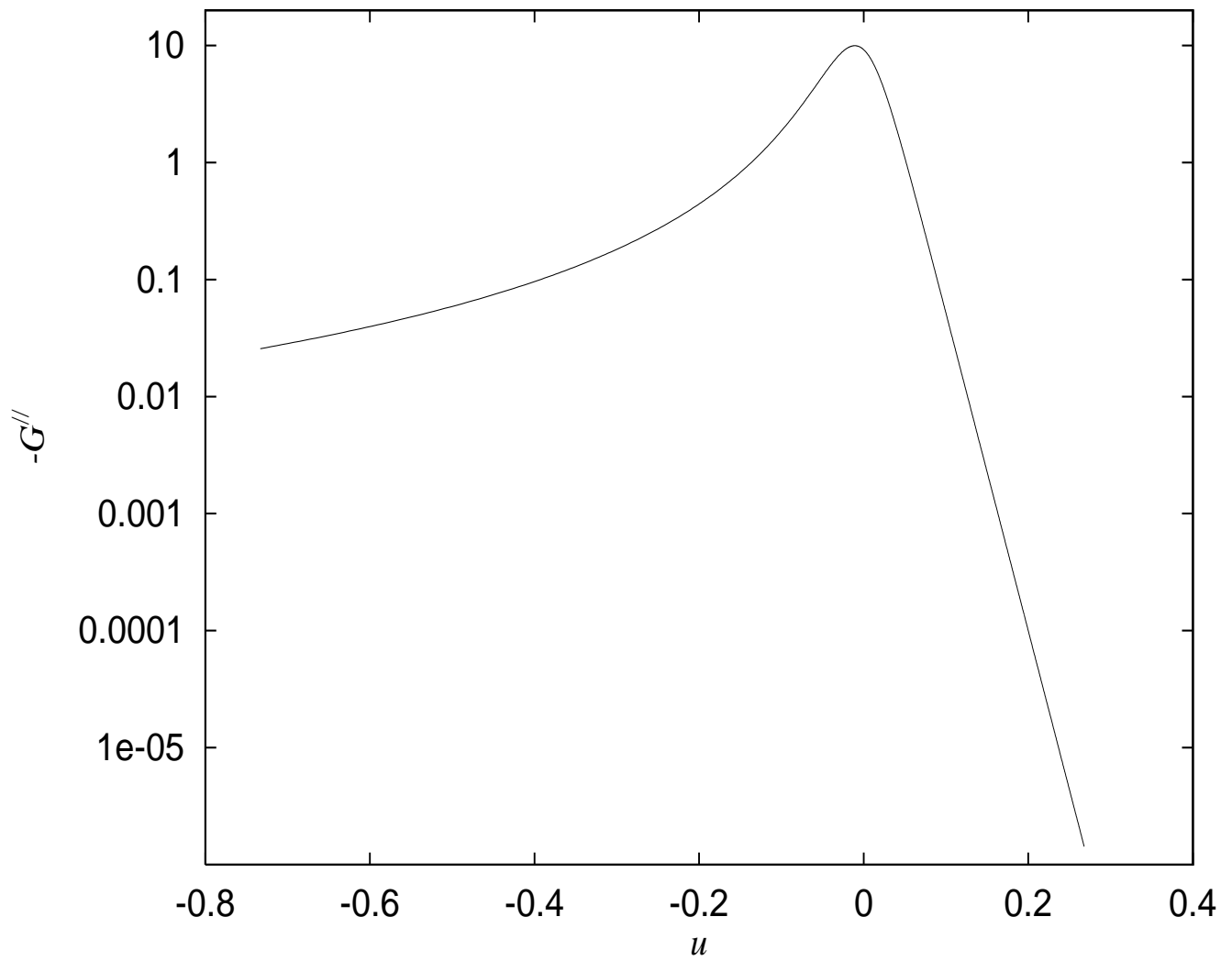
FIG. 4. Null rays interior of the dust cloud in the Oppenheimer-Snyder spacetime.



(a)



(b)



(c)

FIG. 5. Plots of (a) $G(u)$, (b) $G'(u)$, and (c) $G''(u)$ for the Oppenheimer-Snyder spacetime.

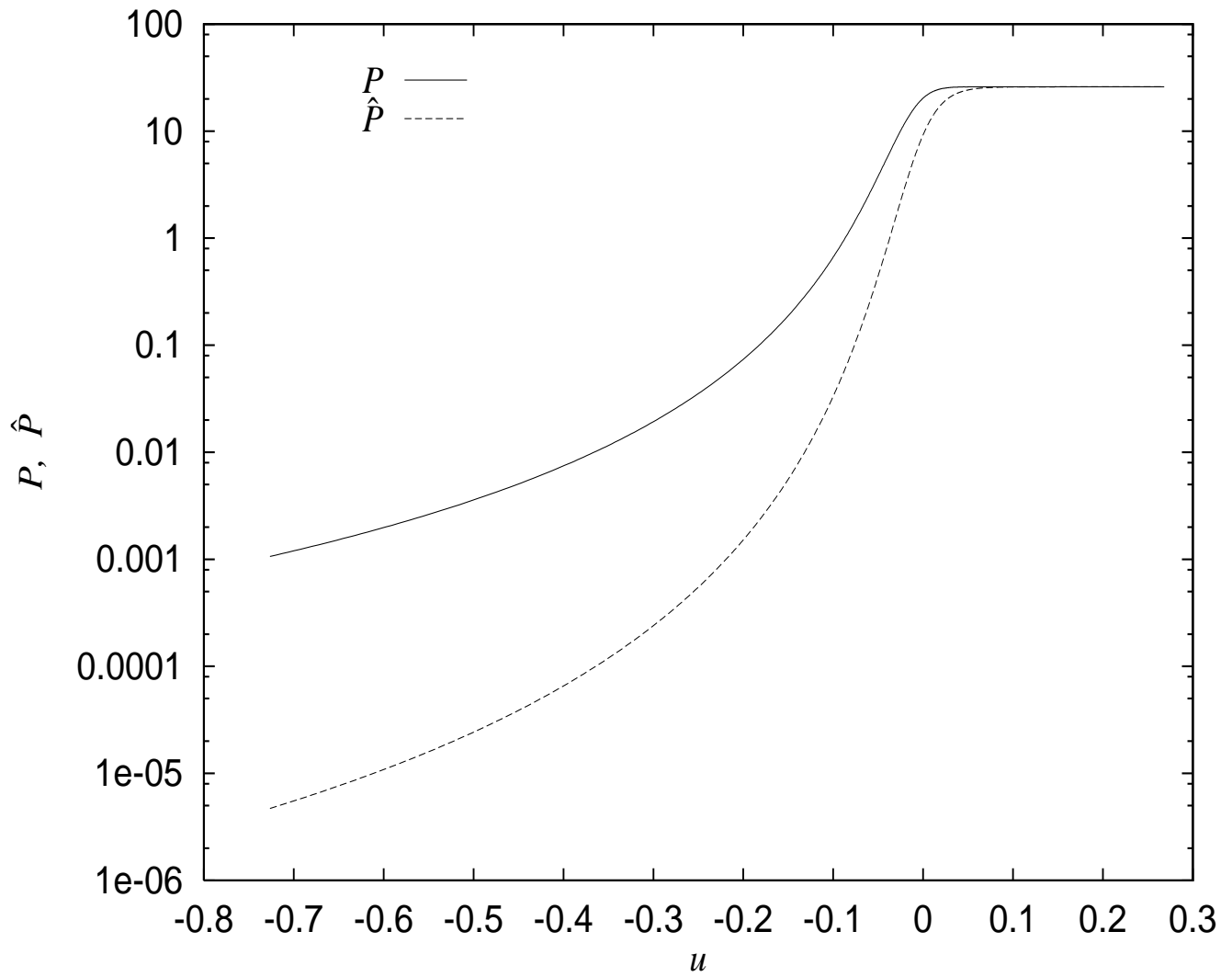


FIG. 6. Power for minimally and conformally coupled scalar fields in the Oppenheimer-Snyder spacetime.

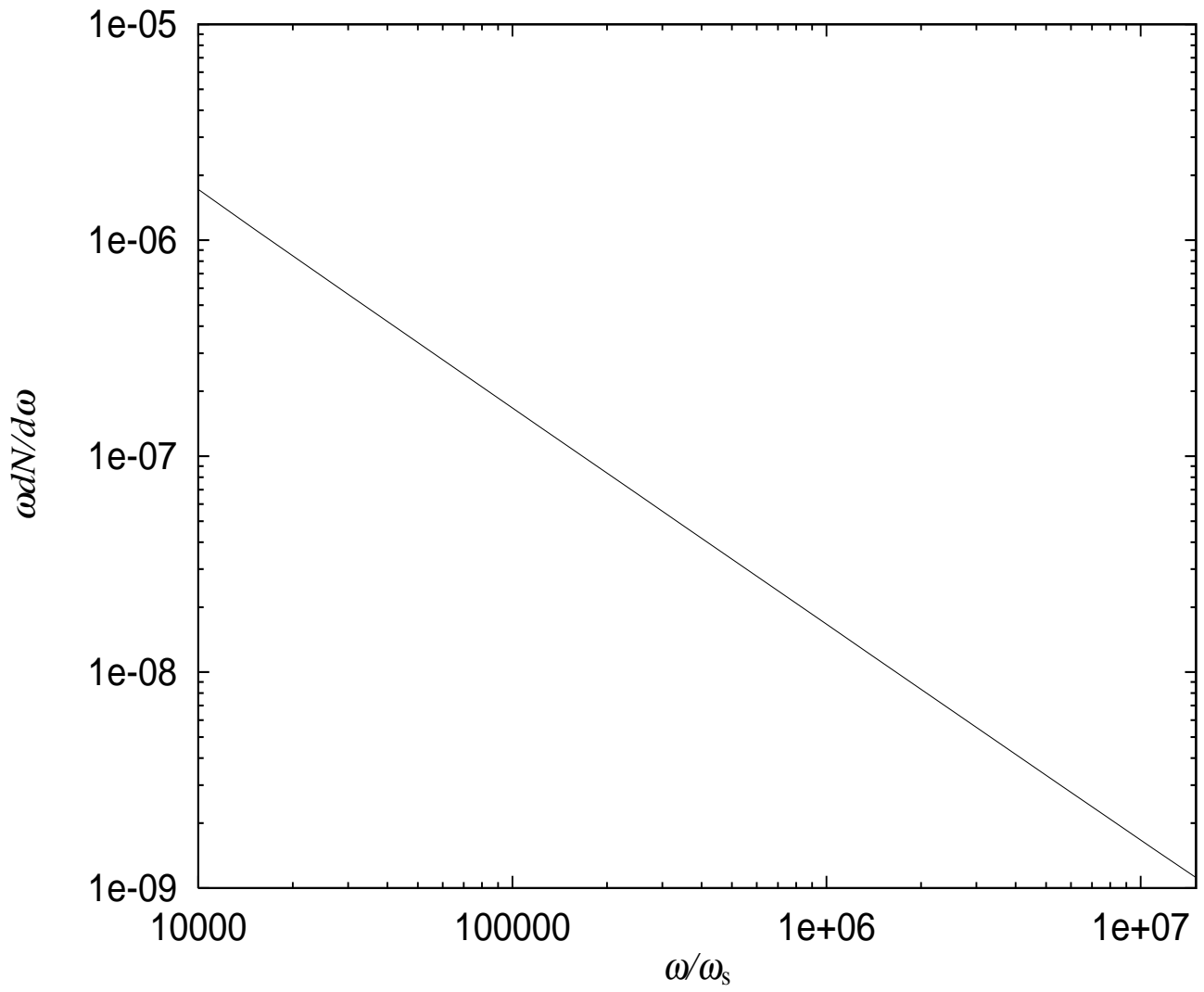


FIG. 7. Total spectrum of a naked singularity explosion for $A = 0.8$ and $f_l = 1$.

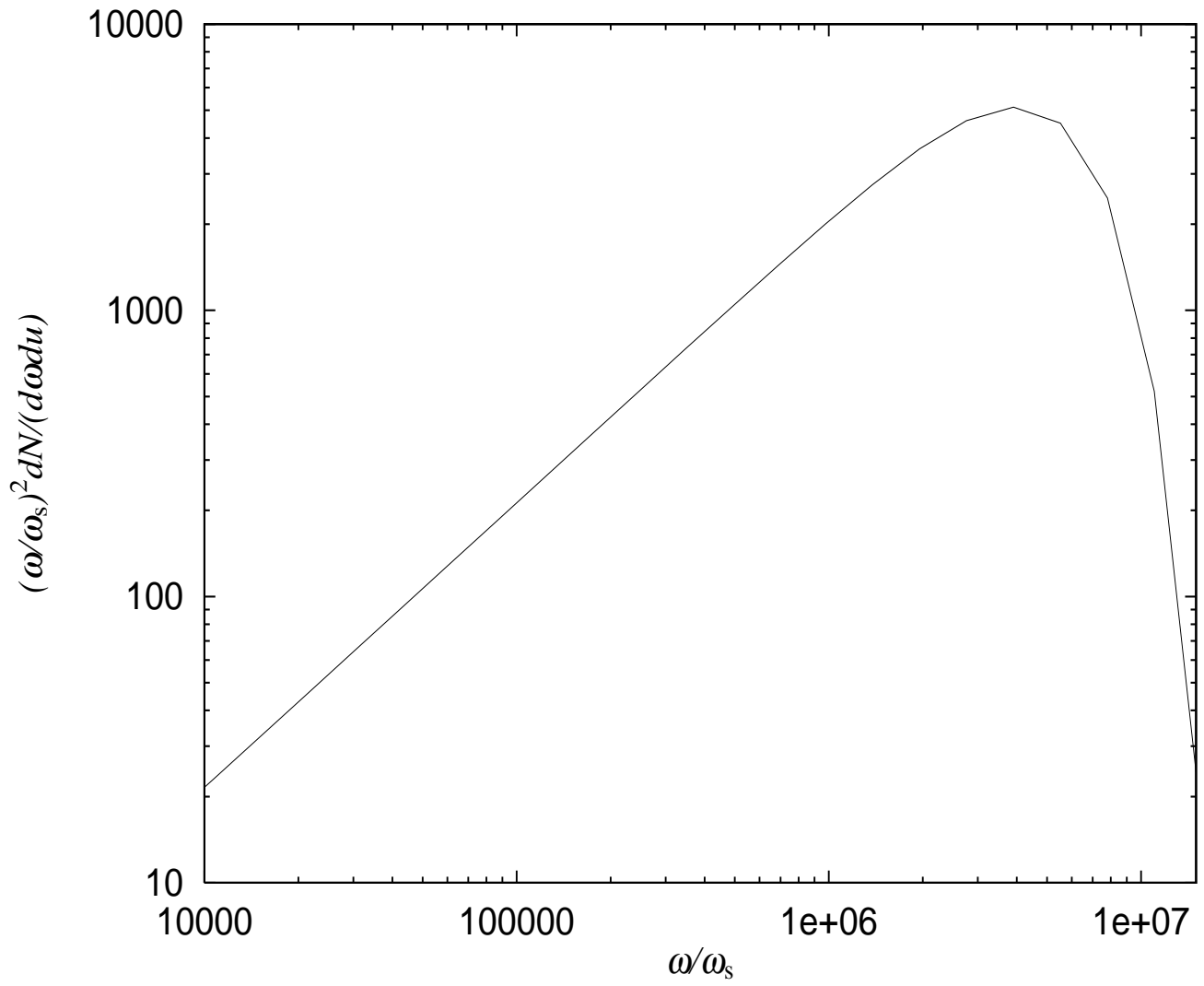


FIG. 8. Momentary spectrum of a naked singularity explosion at $u_0 - u = 10^{-6}\omega_s^{-1}$ for $A = 0.8$ and $f_l = 1$.

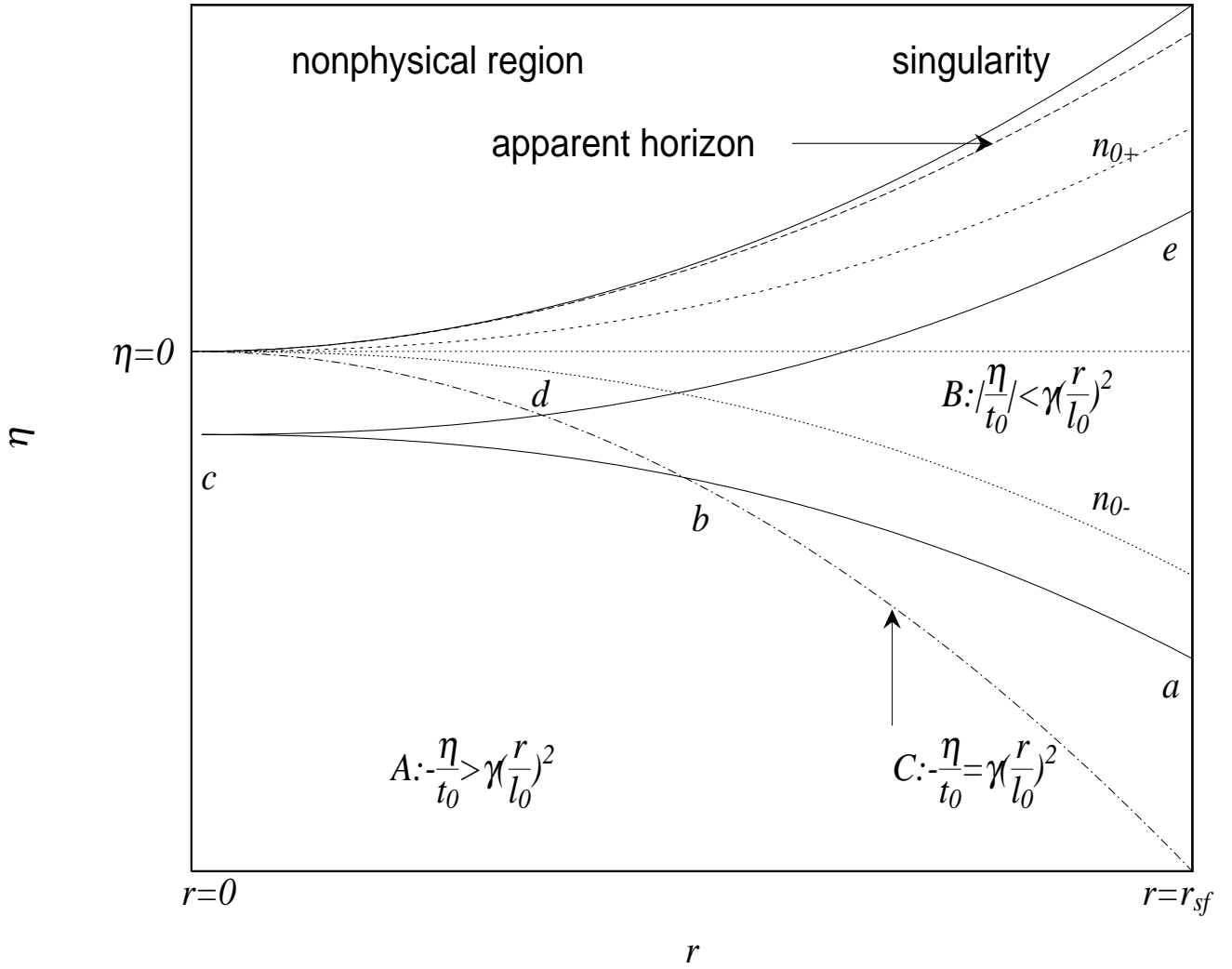


FIG. 9. Schematic diagram of the LTB spacetime interior of the dust cloud around the naked singularity